International Atomic Energy Agency

INDC(CCP)-329/L

INDC INTERNATIONAL NUCLEAR DATA COMMITTEE

TRANSLATION OF SELECTED PAPERS
PUBLISHED IN YADERNYE KONSTANTY (NUCLEAR CONSTANTS 3, 1989)

(Original Report in Russian was distributed
as INDC(CCP)-306/G)

Translated by A. Lorenz
for the
International Atomic Energy Agency

March 1991

IAEA NUCLEAR DATA SECTION, WAGRAMERSTRASSE 5, A-1400 VIENNA

INDC(CCP)-329/L

TRANSLATION OF SELECTED PAPERS

PUBLISHED IN YADERNYE KONSTANTY (NUCLEAR CONSTANTS 3, 1989)

(Original Report in Russian was distributed
as INDC(CCP)-306/G)

Translated by A. Lorenz
for the
International Atomic Energy Agency

March 1991

Reproduced by the IAEA in Austria
April 1991

91-01296

Contents

THE EFFECT OF THE ^{238}U NEUTRON STRENGTH FUNCTION UNCERTAINTY ON RESONANCE STRUCTURE CALCULATIONS IN UNRESOLVED REGIONS

V.N. Koshcheev, G.N. Manturov, V.V. Sinitsa

Abstract

The effect of the neutron strength function uncertainties on the calculated values of the self-shielding factors and energy dependence of the total and capture ^{238}U cross-sections in the unresolved resonance region are investigated.

In actual calculations of the physical characteristics of nuclear reactors it is common practice to use group cross-sections to represent the interaction of neutrons with matter. As a rule, such cross-sections are taken from specially prepared sets of group constants [1,2]. Nowadays, the preparation of group constants consists in the reprocessing of information on the interaction of neutrons with nuclides which are stored in evaluated neutron data files [3,5]. The information used in this procedure consists of detailed descriptions of the energy dependence of cross-sections, resolved resonance parameters, averaged resonance parameters in the unresolved resonance region, etc...

Inasmuch as ^{235}U is the most important fuel material of fast reactors, the knowledge of its group cross-sections is most important in the ≈ 1 to 100 KeV energy region where one observes the neutron spectrum maximum, and which comprises approximately one third of the total number of capture events in the core of a fast reactors. For ^{238}U, this energy region is the region of unresolved resonances. The only experimental data available in this energy region consist of cross-sections averaged over a given spectrum, as well as transmission and self-shielding functions for various sample thicknesses and temperatures.

In calculations, the group cross-section σ_{xg} for the reaction (n,x) in the energy group g, at a material temperature θ, calculated by using a background cross-section σ_0 (parametrizing the dilution by other components of the medium) is

expressed as follows

$$\sigma_{xg}(\theta,\sigma_0) = \sigma_{xg} \cdot f_{xg}(\theta,\sigma_0)$$

where σ_{xg} is the cross-section for the (n,x) reaction at infinite dilution (independent of the temperature of the medium); and

$f_{xg}(\theta,\sigma_0)$ is the resonance self-shielding factor for that reaction (which is determined by the interpolation of f-factors as a function of θ and σ_0 [1]).

According to the request list for nuclear data [6], the accuracy requirements for ^{238}U cross-sections in the ≈ 1 to 100 KeV energy range are as follows: 1 to 2 percent for σ_{tot} and 1 to 3 percent for σ_{cap}. However, current evaluations [7,8] show that the existing accuracies for these cross-sections are far from being satisfied: for σ_{tot} they are approximately 5% and for σ_{cap} they range from 1% to 3%. It must be noted that the values of these reaction cross-sections are determined by measurements, so that the achievement of the required uncertainties depends primarily on the development and improvement of experimental techniques and measurement methods. The cross-section self-shielding factors f_{xg} in the region of unresolved resonances, on the other hand, are determined as a rule with the aid of theoretical models. These calculations require the following average resonance parameters: the average neutron width Γ^l_n and the average radiation width Γ_γ, the average level spacing D_l, and the potential scattering radius R_l (for each ^{238}U nuclear level and for a neutron angular momentum l).

The following accuracies are required for resonance self-shielding factors of the radiative capture cross-section [6]: ≈ 2%-3% for $f_{cap}(300^0K,\sigma_0)$ in the pertinent region of σ_0 for fast reactors (i.e., 10 barns < σ_0 < 100 barns) and is approximately 7% for the Doppler broadening self-shielding factors:

$$\Delta^{cap}(\sigma_0) = f_{cap}(\theta_1,\sigma_0) - f_{cap}(\theta_2,\sigma_0) \approx 7\%$$

However, these requirements have not yet been fulfilled [9].

The accuracy requirement for the total cross-section self-shielding factor which stems from the need to have an accurate description of the neutron leakage from the reactor is not too high

$$\text{for} \quad f_{tot} \ (\sigma_0 > 10 \text{ barns}) \approx 10\%$$

$$\text{and for} \quad \Delta^{tot} \ (\sigma_0 > 10 \text{ barns}) \approx 30\%$$

The accuracies of calculated cross-section self-shielding factors have been evaluated in earlier works [1,10] devoted to the evaluation of average ^{238}U cross-sections and resonance parameters. The average resonance parameters obtained by the authors of these earlier works were calculated on the basis of the method of "maximum likelihood" using experimental information on average cross- sections. The accuracies of cross-section self-shielding factors calculated in this manner proved to be quite high: $\approx$ 1.5% for f_{cap} and $\approx$ 3.0% for f_{tot}.

In this work, an attempt was made to evaluate the accuracies of $f_x(\theta,\sigma_0)$ and $\Delta f_x(\theta,\sigma_0)$ on the basis of other considerations, namely on the assumption of existing uncertainties in the values of resonance parameters.

UNCERTAINTY IN THE AVERAGE RESONANCE PARAMETERS

As indicated above, in order to calculate the self-shielding factors for the cross-section f_{xg}, it is necessary to know the average values of the following resonance parameters: Γ_n^l, Γ_γ, D_l and R_l. It turns out that the influence of these parameters on the calculated value of f_{xg} is not the same. As shown in references [10] and [11], the major constituent of the cross-section self-shielding effect in the energy region of interest consists of the self-shielding of the cross-section for the interaction of neutrons with nuclei which have an orbital angular momentum of l=0 (S-wave), in other words the ability to predict self-shielding cross-sections is limited by uncertainties in ones knowledge of the neutron strength function $S_n^0 = \Gamma_n^0/D$.

The magnitude of the uncertainty in the quantity S_n^0 can be seen in Fig.1, which shows the experimental values of the neutron

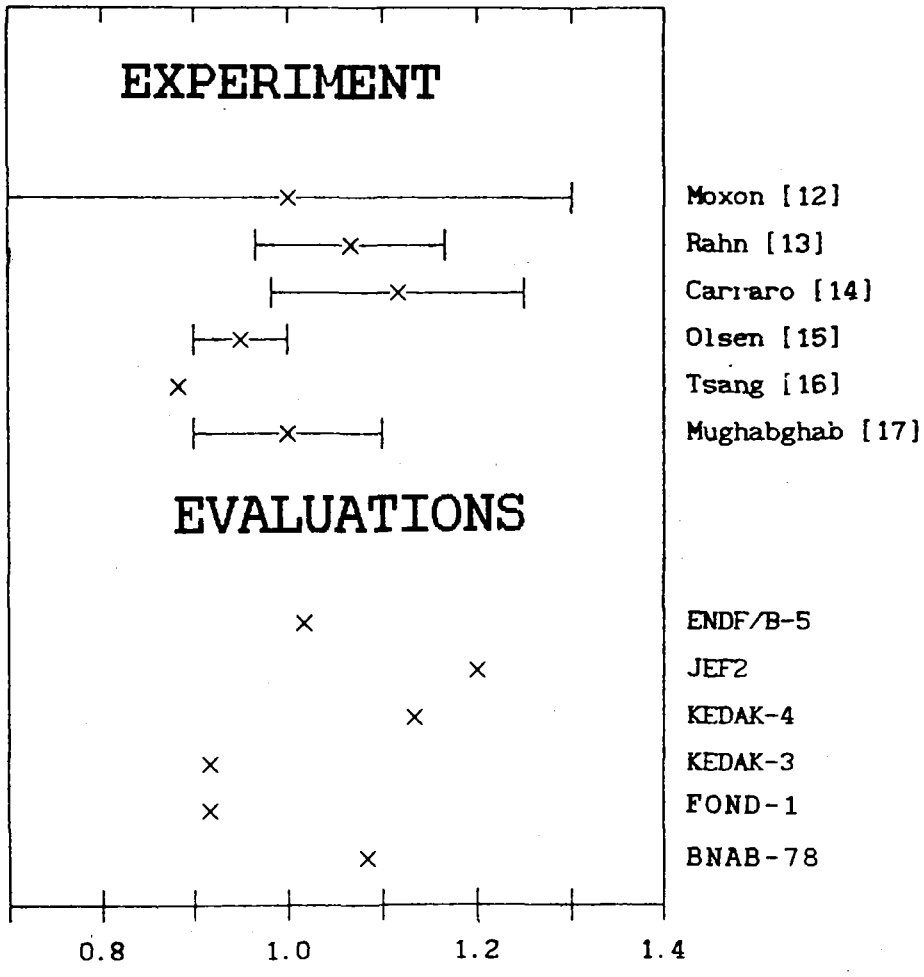

Fig.1. Distribution of the neutron strength function S_n^0 for ^{238}U

strength function determined by individual authors, as well as values adopted by various libraries of evaluated neutron data for ^{238}U. It can be seen that the values of the quantity S_n^0 lie in the interval ranging from 0.9×10^{-4} to 1.2×10^{-4}. The following observation can be made regarding the uncertainties of the other average resonance parameters:

- the experimental value of the S_n^1 function (p-wave) ranges from 1.4×10^{-4} in reference [13] to 2.89×10^{-4} in reference [18];

- the neutron strength function S_n^2 for d-waves has an even broader spread: in the JENDL-2 library the value for this quantity is 1.0×10^{-4}, while reference [7] reports a value of 3.0×10^{-4};

- the potential scattering radius R_0 varies from 8.9 fermi in the ENDF/B-5 library to 9.44 fermi in refrence [15];

- the radiative strength function S_γ is known to a high degree of accuracy: from $(10.3\pm0.6)10^{-4}$ in reference [17] to 11.75×10^{-4} in ENDF/B-5.

It can be seen from this example that of all the average resonance parameters used in the calculation of the quantity f_{xx}, the neutron strength function S_n^0 and the radiative strength function S_γ are known to the highest degree of accuracy. The other resonance parameters exhibit a much broader scatter, and with the exception of the potential scattering radius, they do not require as high a degree of accuracy in the energy range of interest.

CALCULATION OF THE CROSS-SECTION SELF-SHIELDING FACTORS

Based on the premise that the uncertainty in the neutron strength function has a maximum effect on the resonance self-shielding, six values of this quantity were chosen as a first step, namely S_n^0 = 0.9, 1.0, 1.1 and 1.2×10^{-4}, considered to be most plausible, as well as two less likely, extreme values, namely S_n^0 = 0.8 and 1.5×10^{-4}. The other average resonance parameters used in the calculation of the resonance self-shielding effect were then computed with the aid of the EVPAR program [19]. These parameters were then calculated so that the values of the total cross-section σ_{tot} and the radiative capture cross-section σ_{cap} fell within the bounds of their existing uncertainties. The average resonance parameters calculated in this manner are given in the Table below. In addition, the following quantities were calculated for each set of parameters:

- self-shielding factors for the total $f_{tot}(\theta,\sigma_0)$ and capture $f_{cap}(\theta,\sigma_0)$ cross-sections for θ = 300°K and for dilution cross-sections ranging from σ_0 = 0 barn (when the resonance self-shielding effect is at a maximum) to $\sigma_0 = 10^5$ barns (when the resonance structure is completely masked by the cross-section structure of the other nuclides in the medium);

- corresponding Doppler broadening effect on the self-shielding of the cross-sections (n,x) at higher temperatures:

$$\Delta_1^x(\sigma_o) = f_x(900K, \sigma_o) - f_x(300K, \sigma_o)$$

$$\Delta_2^x(\sigma_o) = f_x(2100K, \sigma_o) - f_x(900K, \sigma_o)$$

These values were computed using the program PPP GRUKON [20].

Sets of Average Resonance Parameters for ^{238}U

P/P	l	S_n^l, 10^{-4}	S_γ^l, 10^{-4}	R_l, fermi
1	1	1.65	8.75	4.59
	2	1.46	11.40	9.24
2	0	0.90	13.30	9.53
	1	1.82	8.55	5.00
	2	1.77	11.30	9.24
3	0	1.00	12.10	9.38
	1	2.00	8.34	5.40
	2	2.11	11.30	9.24
4	0	1.10	11.10	9.22
	1	2.18	8.17	5.74
	2	2.41	11.40	9.24
5	0	1.20	10.20	9.06
	1	2.37	8.00	6.09
	2	2.73	11.50	9.24
6	0	1.50	7.42	8.48
	1	3.16	7.79	5.82
	2	3.35	12.80	9.24

CALCULATION RESULTS AND DISCUSSION

The energy dependences of the total cross-section σ_{tot}, the radiative capture cross-section σ_{cap} and their corresponding relative values (where the value of $S_n^0 = 1.1 \times 10^{-4}$ was taken as the basis), obtained by using different sets of average resonance parameters, are shown in Fig.2. It can be seen that the radiative capture is reproduced very well for all sets of parameters, incurring variations not exceeding ≈3%. Although the

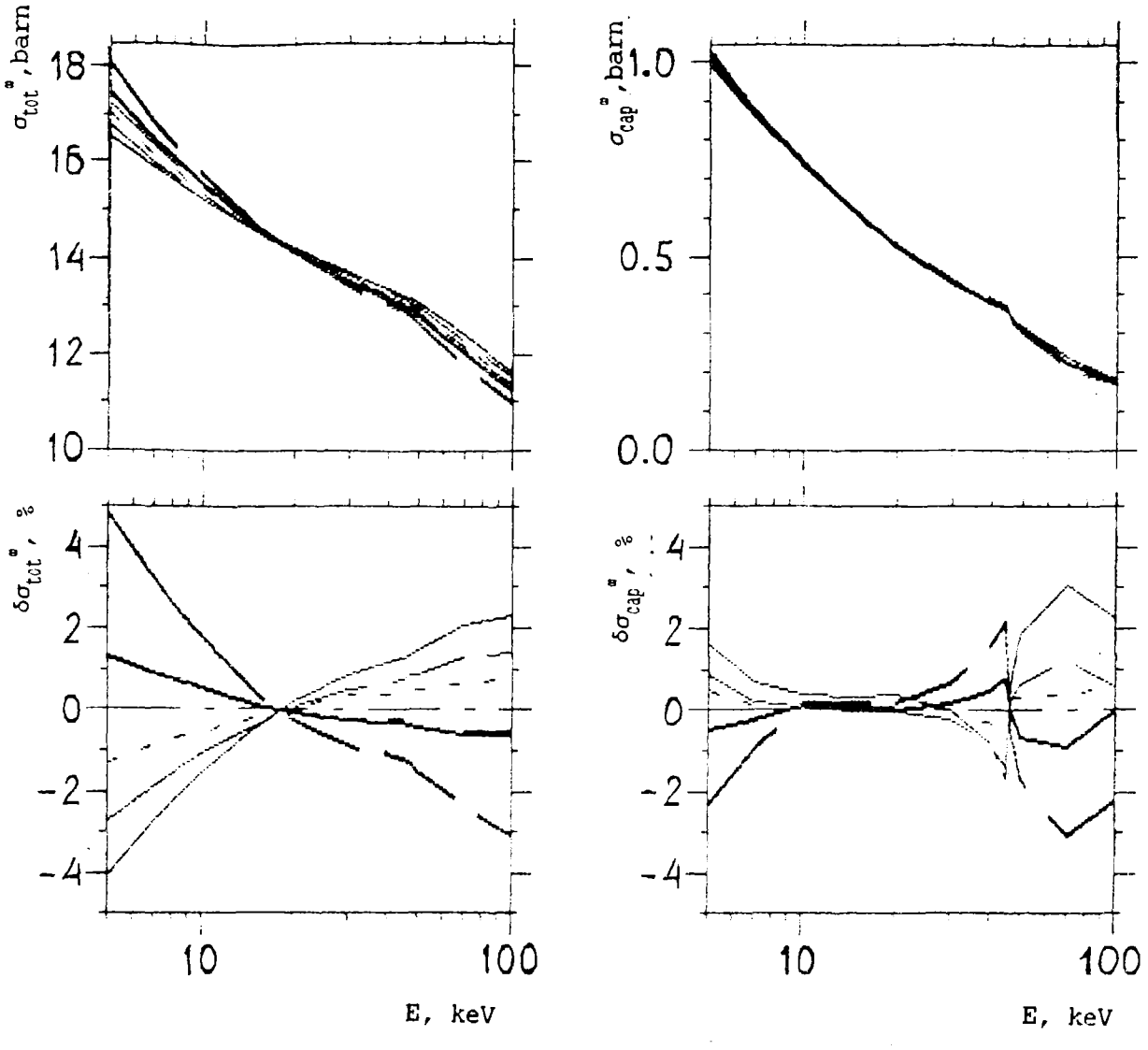

Fig.2. Total cross-section and radiative capture cross -section for ^{238}U for different values of the neutron strength function:

——— - $S_n^o=0.8\cdot10^{-4}$; —— —— - $S_n^o=0.9\cdot10^{-4}$;
— — — - $S_n^o=1.0\cdot10^{-4}$; — - — - $S_n^o=1.1\cdot10^{-4}$;
═══ - $S_n^o=1.2\cdot10^{-4}$; ═══ ═══ - $S_n^o=1.5\cdot10^{-4}$

total cross-section diverged more for the various sets of average resonance parameters than in the case of σ_{cap}, its values do not exceed the bounds of experimental accuracy of ≈4%.

A similar behavior can also be observed for the cross-section self-shielding factors. Thus, the quantity f_{cap} can be calculated reliably using any of the resonance parameter sets. For $S_n^0 = 0.8x10^{-4}$, the maximum spread in the data exceeds ≈1% only slightly (see Fig.3, which shows the energy dependence of the absolute and relative values of $f_{cap}(300K,0)$ and the

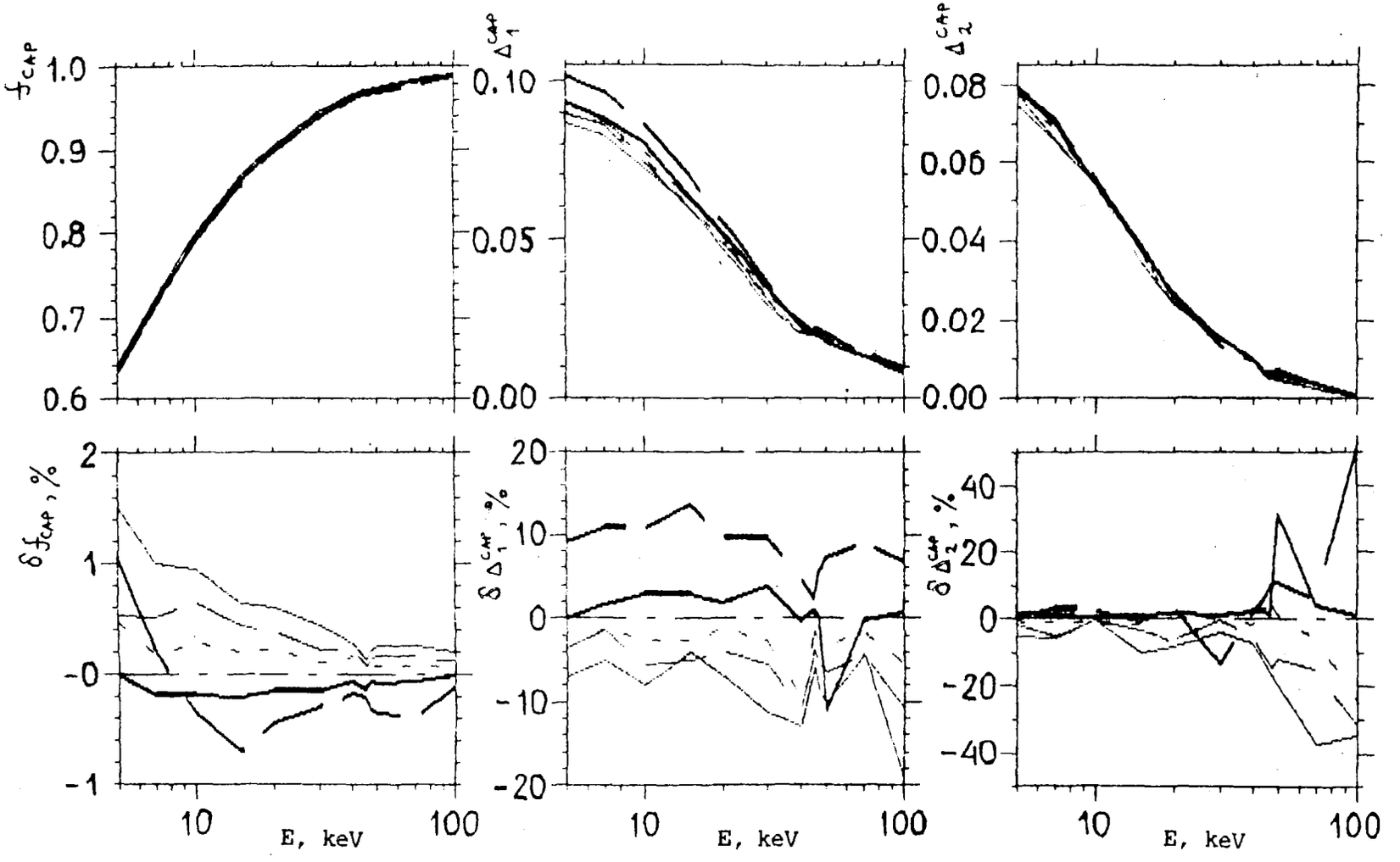

Fig.3. Self-shielding factors for the radiative capture cross-section and the corresponding Doppler effects for σ_0 = 0 barns:
S^0_n = 0.8x10^{-4} ——— , S^0_n = 0.9x10^{-4} —— —— —— ,
S^0_n = 1.0x10^{-4} — — — , S^0_n = 1.1x10^{-4} – —— – —— ,
S^0_n = 1.2x10^{-4} ═══, S^0_n = 1.5x10^{-4} ═ ═ ═

corresponding quantity $\Delta^{cap}(0)$. The effect of Doppler broadening on the radiative capture cross-section self-shielding is reproduced very well in the lower end of the energy range, where the maximum scatter is approximately 10%. The divergence of these values increases at higher energies, where even the magnitude of the absolute values of the broadening become small. In this energy region the values of the cross-section self-shielding factors approach unity; Doppler broadening (like the difference between two closely-lying values) becomes a very sensitive factor in the accuracy of the calculation of the $f_{xs}(\theta,\sigma_0)$, which is calculated to an accuracy of two to three decimal points.

As the dilution cross-section σ_0 increases, the scatter of the reconstituted values of $f_{cap}(\theta,\sigma_0)$ calculated with the various sets of resonance parameters becomes smaller. Thus, for $\sigma_0 \approx 100$ barns, the divergence in the values of $f_{cap}(300K,10)$ is approximately 1%, and for Δ^{cap} it is ≈3%.

The value of the total cross-section self-shielding factor, however, is strongly dependent on the resonance parameter set used in the calculation (see Fig.4). The divergence in the values of f_{tot} for $\sigma_0 = 0$ barns varies from 30% in the lower energy region to ≈5% in the upper energy region. As the value of the dilution cross-section σ_0 increases this divergence decreases; for $\sigma_0 = 10$ barns, the scatter is approximately 15%, and for
$\sigma_0 = 10$ barns it is ≈10%. Fig.4 shows that for a σ_0 value of 10 barns, Doppler broadening is also strongly dependent on the resonance parameter set used. The divergence in the relative values do not change significantly with the increase in the value of the dilution cross-section σ_0.

The difference in the behavior between the total and radiative capture cross-section self-shielding factors can be explained by the nature of these two individual processes. The radiative capture process is described primarily by p-wave parameters, while the total interaction is described by s-wave parameters. However, as it has already been mentioned above, the contribution of the p-wave to the cross-section self-shielding

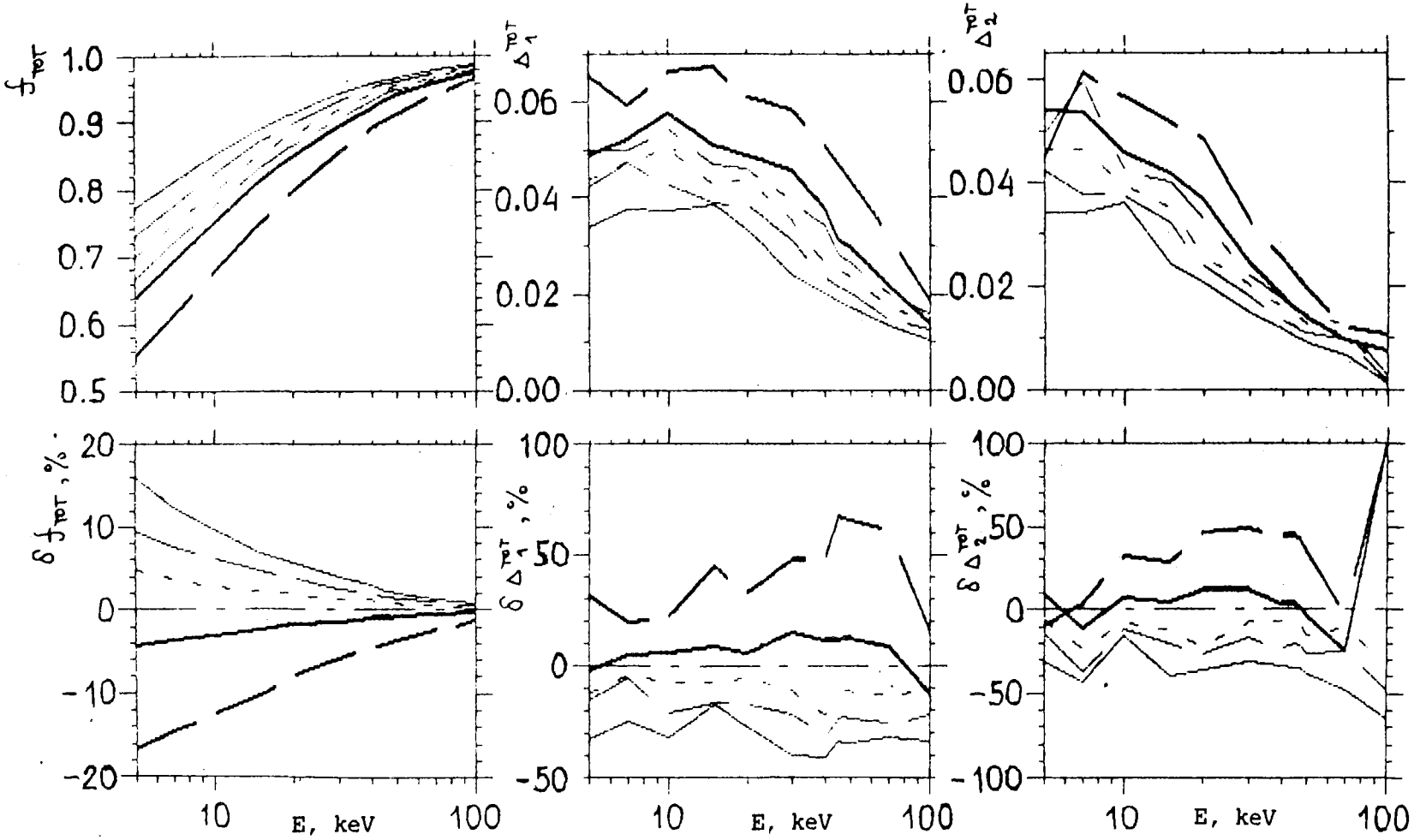

Fig.4. Self-shielding factor for the total cross-section and corresponding Doppler broadening effects for σ_0 = 10 barns:
S^0_n = 0.8x10^{-4} ——— , S^0_n = 0.9x10^{-4} — — — , S^0_n = 1.0x10^{-4} — — — , S^0_n = 1.1x10^{-4} — — — — , S^0_n = 1.2x10^{-4} ═══, S^0_n = 1.5x10^{-4} ═ ═ ═

effect is considerably smaller than that of the s-wave. Furthermore, the additional S_γ parameter is included in the calculation of the radiative capture self-shielding effect [10] at a point where the sensitivity coefficient of f_{tot} to the change in the value of the S_γ parameter is equal to zero.

The analysis described above took into account calculational results based on all sets of resonance parameters, including those based on the extreme values of $S_n^0 = 0.8 \times 10^{-4}$ and 1.5×10^{-4}. The observed divergence becomes much smaller if one ignores these two extreme cases. Consequently, it can be deduced that the existing uncertainties in the neutron strength function S_n^0 have a weak influence on the calculated radiative capture cross-section self-shielding factor $f_{cap}(\theta,\sigma_0)$; on the other hand, the value of the total cross-section self-shielding factor $f_{tot}(\theta,\sigma_0)$ does depend on the value of S_n^0, but its accuracy requirements are satisfied by the existing uncertainties in S_n^0.

The question is, what is the reliability of the evaluated cross-sections and of the average resonance parameters in the energy region of unresolved resonances? With regard to the radiative capture cross-section, the recently observed tendency in the decrease of its values [21,22] seem to indicate that early experimental measurements of the radiative capture cross-section evidently included systematic errors. One such error arises as a result of the incorrect consideration of multiple scattering of neutrons in the sample [23].

The total cross-section is determined by extrapolating the observed cross-section $\sigma_{obs}(n) = -\ln(T_n)/n$ (where n is the sample thickness and T_n the transmission parameter) to a zero sample thickness. The difficulties in such a procedure can be judged from Fig.5, which shows a plot of experimental values and calculated curves of $\sigma_{obs}(n)$ at an energy of ≈7 keV. Inasmuch as the value of the neutron strength function S_n^0 is derived from the lower region of the $\sigma_{obs}(n)$ curve, the uncertainties in the experimental data in that region do not allow an accurate determination of the S_n^0 quantity. Therefore, if a more accurate value of the neutron strength function is desired, it is essential to have reliable experimental transmission function

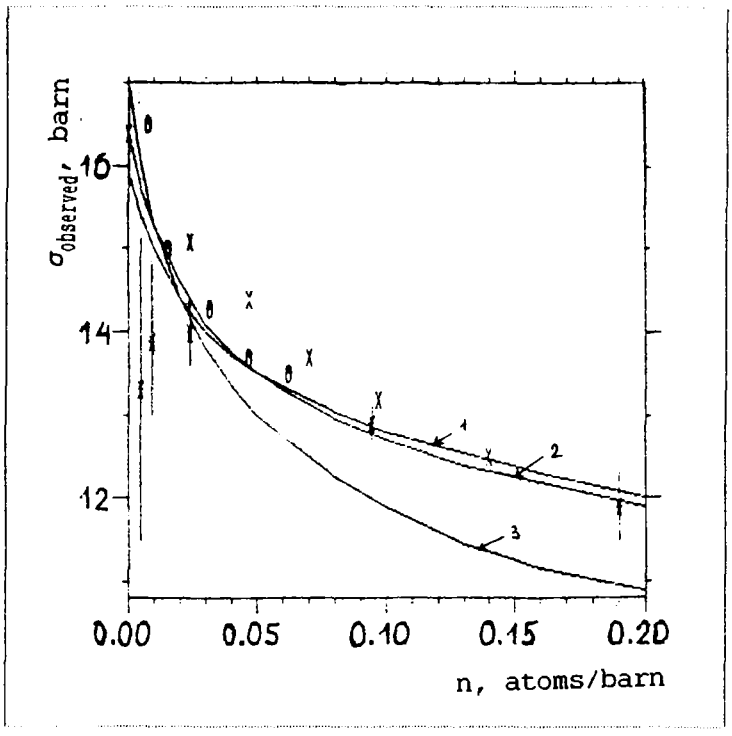

Fig.5. The dependence of σ_{obs} on sample thickness, where

1 - calculation with $S_n^0 = 0.93 \times 10^{-4}$
2 - calculation with $S_n^0 = 1.1 \times 10^{-4}$
3 - calculation with $S_n^0 = 1.5 \times 10^{-4}$

θ - data from Ref.[24]
* - data from Ref.[25]
x - data from Ref.[26]

data for $n \to 0$ as input for such an analysis rather than relying on the values of extrapolated cross-sections.

REFERENCES

[1] ABABYAN, L.N., BAZAZYAN, N.O., NIKOLAEV,M.N., TSIBULYA,A.M., Group Constants for Reactor and Shielding Calculations, Ehnergoizdat, Moscow (1981) (in Russian).

[2] TAKANO,H., et al., JAERI Fast Reactor Group Constants Set (ver.2), Rep. JAERI-1255 (1978).

[3] NATIONAL NUCLEAR DATA CENTER, ENDF/B Summary Documentation (comp. by R.Kinsey), Rep. BNL-17541 (ENDF-201), 3rd Ed. (1979).

[4] BLOKHIN, A.I., et al., in: Nejtronnaya Fizika: Proc. First International Conference on Neutron Physics, Kiev, 14-18 October 1987, Vol.1, TsNIIatominform, Moscow (1988) 45 (in Russian).

[5] JAPANESE NUCLEAR DATA CENTER, Japanese Evaluated Nuclear Data Library, JENDL-1, ver.1, Rep. JAERI-1261 (1979).

[6] INTERNATIONAL ATOMIC ENERGY AGENCY, World Request List for Nuclear Data 1987-1989 (WANG DAHAI, Ed.), Rep. INDC(SEC)-095 (1988).

[7] MANTUROV, G.N., LUNEV, V.P., GORBATCHEVA, L.V., in: Nejtronnaya Fizika: Proc. Sixth All-Union Conference on Neutron Physics, Kiev, 2-6 October 1983, Vol.2, TsNIIatominform, Moscow (1984) 231 (in Russian).

[8] SOWERBY, M.G., BEE, N.J., (Proc. IAEA Consultants Mtg on U and Pu Isotope Resonance Parameters, Vienna, 1981), Rep. INDC(NDS)-129 (1982) 136.

[9] KOSHCHEEV, V.N., TSIBULYA,A.M., in: Nejtronnaya Fizika: Proc. First International Conference on Neutron Physics, Kiev, 14-18 September 1987, Vol.1, TsNIIatominform, Moscow (1988) 45 (in Russian).

[10] KOSHCHEEV, V.N., MANTUROV, G.N., NIKOLAEV, M.M., SINITSA, V.V., in: Nejtronnaya Fizika: Proc. Sixth All-Union Conference on Neutron Physics, Kiev, 2-6 October 1983, Vol.1, TsNIIatominform, Moscow (1984) 103 (in Russian).

[11] ABAGYAN, L.P., et al., in: Problems of Atomic Science and Technology. Ser. Nuclear Constants, Vol.8(1), TsNIIatominform, Moscow, (1972) 154 (in Russian).

[12] MOXON, M.C., Sc. Thesis (1968).

[13] RAHN, F., et al., Phys. Rev. C6 (1972) 1854.

[14] CARRARO, G., KOLAR, W., in Proc. Third Conference on Neutron Cross-Sections and Technology, Knoxville, TE. (1971) 70.

[15] OLSEN, K.D., et al., Nucl. Sci. and Eng. 62 (1977) 479.

[16] TSANG, F.Y., BRUGGER, R.M., Nucl. Sci. and Eng. 72 (1979) 34.

[17] MUGHABGHAB, S.F., DIVEDEENAM M., HOLDEN, N.E., "Neutron resonance parameters and thermal cross-sections", Neutron Cross-sections, Vol.1, Part A, Academic Press, New York (1981).

[18] HOUAT, G., et al., Rep. CEA-N-2197 (1981).

[19] MANTUROV, G.N, NIKOLAEV, M.N., Proc. First International Conference on Neutron Physics, Kiev, 14-18 September 1987, Vol.1, TsNIIatominform, Moscow (1988) 440 (in Russian).

[20] SINITSA, V.V., RINEYSKIY, A.A., ibid., p.439 (in Russian).

[21] ADAMCHUK, Yu.V., et al., ibid., Vol.2, p.242 (in Russian).

[22] KAZAKOV, L.E., et al., in: Problems of Atomic Science and Technology. Ser. Nuclear Constants, Vol.3., TsNIIatominform, Moscow (1986) 37 (in Russian).

[23] ANDROSSENKO, A.A., et al., Proc. First International Conference on Neutron Physics, Kiev, 14-18 September 1987, Vol.2, TsNIIatominform, Moscow (1988) 343 (in Russian).

[24] BYOUN, T.Y., BLOCK, R.C., SEMLER, T., Proc. National Topical Meeting on New Developments in Reactor Physics Shielding, USAEC, Lake Kiamesha, New York, September 12-15 (1972) 115.

[25] BOKHOVKO, M.B., et al., in: Problems of Atomic Science and Technology. Ser. Nuclear Constants, Vol.3., TsNIIatominform, Moscow (1988) 11 (in Russian).

[26] PHILIPPOV, V.V., ibid., Vol.4 (1985), p.33 (in Russian).

SIMULTANEOUS EVALUATION OF THE LEVEL EXCITATION FUNCTION AND OF THE GAMMA RAY SPECTRUM FOR INELASTIC SCATTERING OF NEUTRONS ON ^{93}Nb

V.G. Pronyaev, T.S. Belanova, A.I. Yelokhin, A.B. Ignatyuk

Abstract

The level excitation function and the secondary gamma ray spectra from neutron inelastic scattering on ^{93}Nb have been evaluated for the BROND neutron cross-section library.

The possible utilization of niobium as a structural material in the construction of fusion power reactors has stimulated a large number of measurements and calculations of its nuclear characteristics, primarily of its neutron cross sections and spectra of secondary particles generated as a result of its interaction with neutrons.

However, the evaluated neutron data files which were created in the 1970's are not complete. As an example, the information on the level excitation functions for the inelastic scattering of neutrons is available only for the first discrete levels or for groups of these levels; also, the spectra of secondary gamma rays are often represented as a function of temperature even for low energy neutrons, that is when the discrete structure of the spectrum plays a significant role. As a result, the niobium file of the BROND [1] library, which served as the basis for its evaluation at the Technical University of Dresden (TUD, GDR), has been subjected to a substantial review. As one of its prime objectives this review re-evaluated the excitation of levels due to inelastic scattering and the spectra of secondary neutrons and gamma rays.

The evaluated values of the low lying discrete levels of ^{93}Nb, which are given in references [2] and [3], were taken as the basis for this decay scheme. If the spins and parities of some of the levels, given in these references, were either not listed or their values were doubtful, these quantities were determined from the best description of observed neutron inelastic

scattering cross sections calculated by the statistical theory of nuclear reactions. The values of the level energies, their spins and parities, as well as the gamma transition probabilities between levels, all of which are needed in the calculation of gamma ray spectra, and which are in agreement with the data given in reference [20], are presented in the Table below.

More than thirty publications reporting measurements of inelastic scattering cross sections for the excitation of individual levels have been taken into consideration in this evaluation. Two methods were used to perform these measurements: by the direct measurement of the inelastically scattered neutrons using the time-of-flight method [4-12,14,15], or by measuring the gamma ray yield from inelastically scattered neutrons [13,16-23]. As both of these methods are relative, the absolute values of the cross section were determined by using the following standard reaction cross sections: the cross section for the elastic scattering of neutrons on hydrogen or carbon for the direct measurement method, and the cross section of the neutron inelastic scattering for the 845 keV energy level of ^{56}Fe for the gamma ray yield measurement method.

The comparative analysis of the experimental data for each of the excited level of ^{93}Nb was preceded by the normalization of the neutron scattering cross section to the following standards. The partial cross sections from references [4, 8-12] were normalized to the inelastic scattering cross section of ^{56}Fe for the 845 keV level [28]. The data reported in references [4, 8-12] were not renormalized because the standard used in their measurement was the hydrogen elastic scattering cross section taken from one and the same set of evaluated data published in reference [27].

The analyzed experimental neutron inelastic scattering data for the first seven levels of niobium are shown in Fig.1. Also shown on the same figure are the calculated cross sections using the statistical theory computer code ABAREX [29] with consideration given to the fluctuation and correlation of neutron widths.

Some of the partial cross sections were not included in this analysis for the following reasons: measurements by the direct

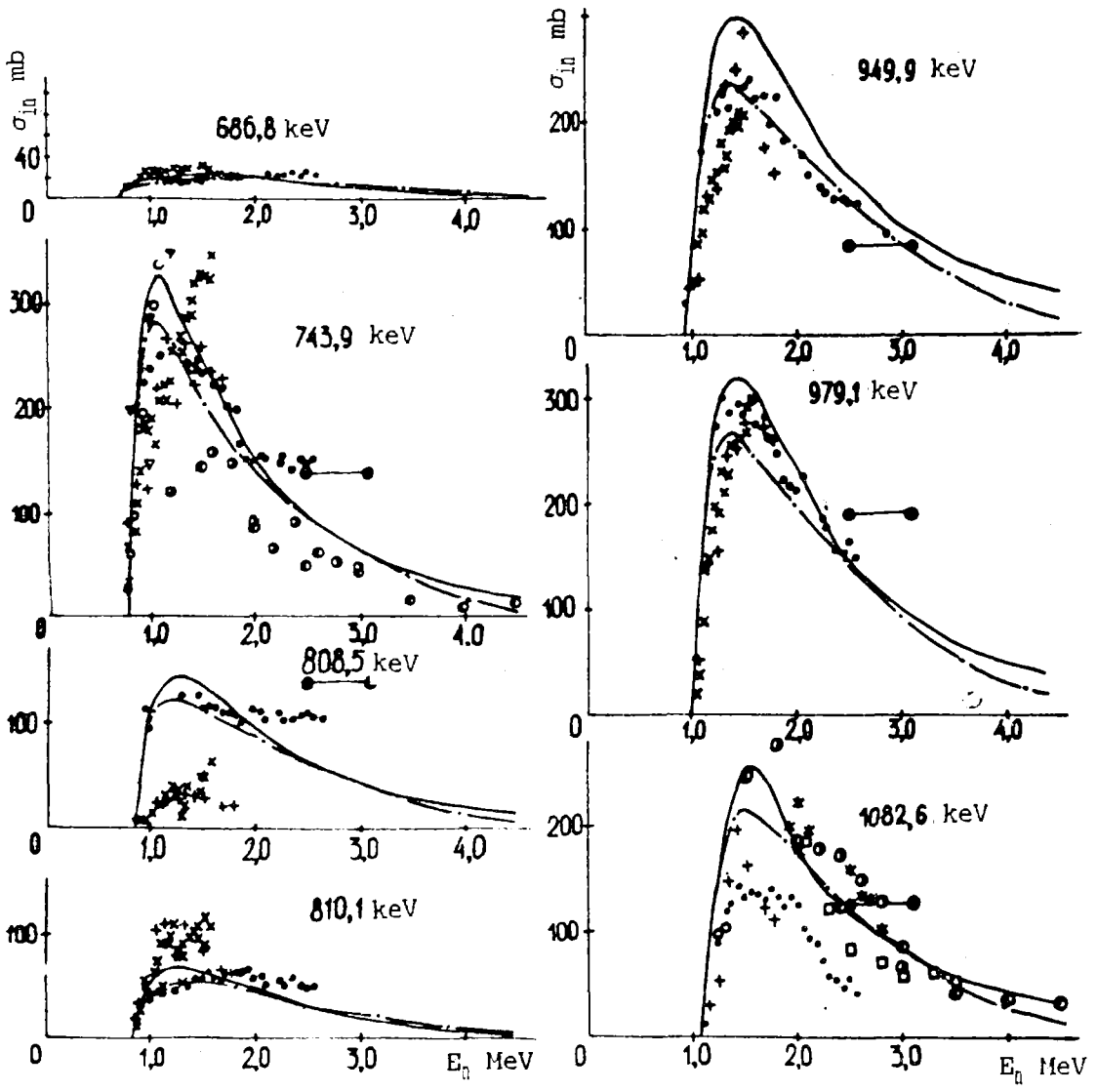

Fig. 1. Excitation functions for the resolved levels of the inelastic scattering of neutrons on ^{93}Nb.
Results of this evaluation ——— , JENDL-3 evaluation — · — .
Experimental data: ○ [4], * [5], □ [8], ⊗ [13], [16,17], ▽ [18], ● [20], + [21], x [22], ▼ [25]

detection of inelastically scattered neutrons using the time-of-flight method yields good results within a limited neutron energy range; the low energy resolution of spectrometers (from 50 to 150 keV) does not always guarantee good enough separation between scattered neutrons from neighboring levels of the excited nuclei. Consequently, part of the data given in references [4-7] represent combined neutron inelastic scattering cross sections for doublets. The only levels which could be resolved, and which were actually used in this evaluation, were the 744 keV [4] and the 1083 keV [4,5,8] energy levels.

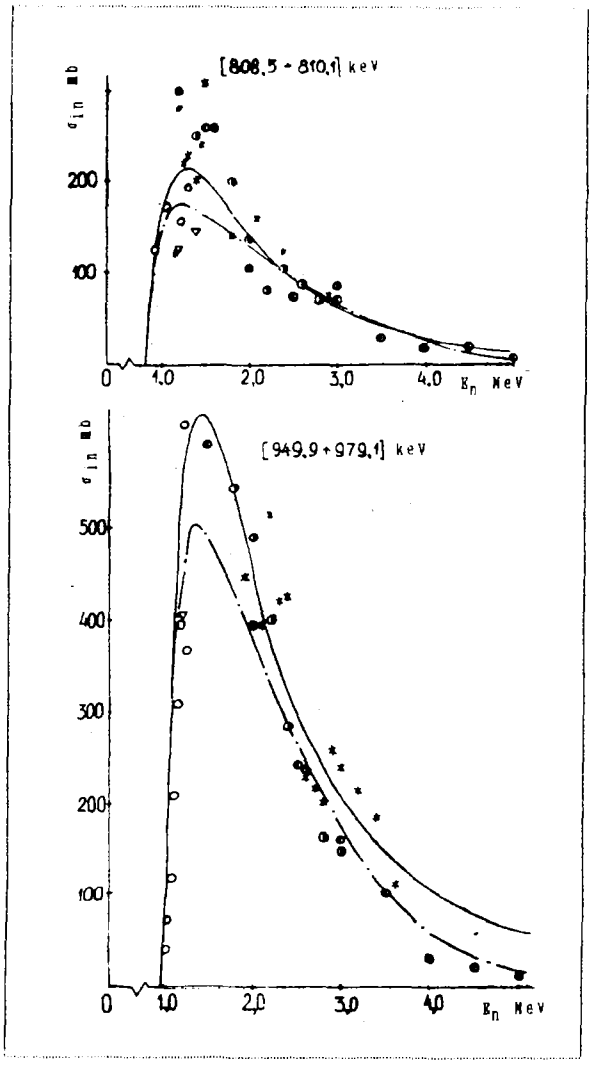

Fig. 2. Excitation function of the unresolved levels of ^{93}Nb for neutron inelastic scattering: results of this evaluation ———— , JENDL-3 [30] evaluation —— . —— ; experimental data: ● [4], * [5-7], O [16-17], ▽ [18]

The inelastic scattering cross sections for the unresolved levels of niobium for the 808-810 keV energies [4,6,7,16,18] and for the 950-979 keV energies are shown in Fig. 2. The corresponding calculated data for the same doublets are also given in this figure.

The method used to measure gamma ray emissions accompanying neutron inelastic scattering has a high energy resolution (≈3 keV for gamma ray energies of 1 MeV [20] and 4.5 keV for ^{60}Co gamma rays [22]), which permits determination of the inelastic scattering cross sections for specific levels to a high degree of accuracy. For each nuclei there is an upper neutron energy limit (for ^{93}Nb it is 1.3 - 1.5 MeV) above which the gamma ray energy spectrum becomes so complex that it is extremely difficult to determine the probability of transition to a given level, and leads to the distortion of the cross section value. As a result,

the partial cross sections for neutron energies larger than 1.3 MeV in the case of data given in references [16-18] and larger than 1.6 MeV in the case of data given in reference [22], were not used in this analysis. As it has been impossible to determine the reason for the considerably large inelastic scattering cross section values given in reference [19], the data from this reference has not been included in the evaluation either.

Occasionally, the method of inverse spherical geometry, which is normally used to measure the cross section for all inelastic events, is used to measure the $\sigma(n,n')$ cross section [25,26]. If the reaction cross sections for the production of charged particles and for neutron capture are considerably smaller in the neutron energy range of interest, then the cross section for the inelastic events is practically the same as the total inelastic scattering cross section. These conditions hold true for niobium and the data given in references [25,26] are therefore taken to be equal the total neutron inelastic scattering cross sections (see Fig. 3).

Although this is an absolute measurement method which is insensitive to the concurrent gamma radiation, it does have a very low energy resolution which limits its application to the measurement of integral cross sections.

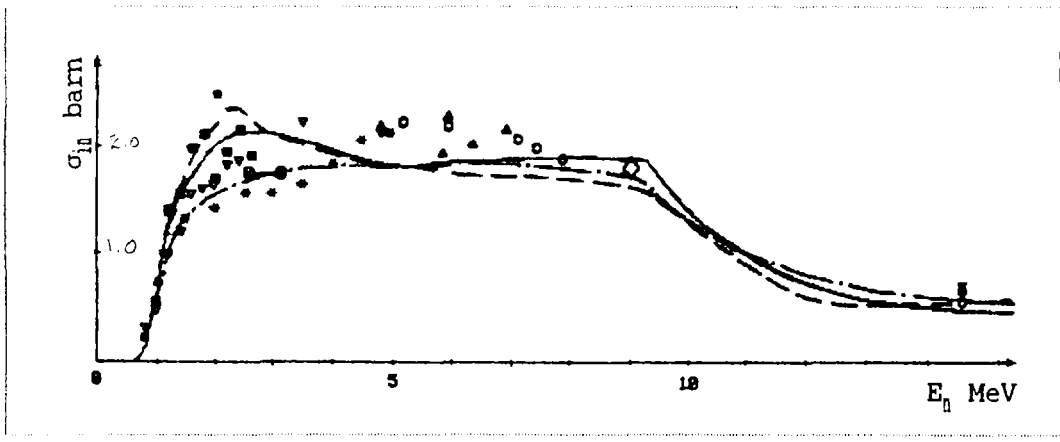

Fig.3. Total neutron inelastic scattering cross section for ^{93}Nb. Results of this evaluation: ———; JENDL-2 [30] evaluation: — · —; BROND [1]: — — — ; experimental data: * [4], □ [10], ○ [12], ⊗ [13], + [14], x [15], ▽ [18], ● [20], ▾ [25], ■ [26], ⊕ [37], ▲ [23], △ [24], ◆ [9]

Total neutron inelastic scattering cross sections for ^{93}Nb in the neutron energy range of 0.8 to 15.0 MeV, obtained from measurements [14,15,24-26] and from calculations using partial cross sections [4,9-13,18,20,23], are shown in Fig.3. The individual cross sections are in good agreement with each other within 10-15%, and are well described by the theoretical curve.

The statistical theory calculations in the continuum range for energy levels above 1.7 MeV were performed using level density data for the Fermi-gas model and parameters from reference [31]. Neutron transmission coefficients were calculated with the use of the spherical optical model using optical potential parameters from reference [32], obtained from the simultaneous analysis of the total and scattering cross section data.

It was assumed that the following levels (E_j=744 keV, J^π=7/2$^+$; E=808.7 keV, J^π=5/2$^+$; E=949.9 keV, J^π=13/2$^+$; E_j=979.1 keV, J^π=11/2$^+$ and E^j=1082.6 keV, J^π=9/2$^+$) are members of a multiplet which combines the single phonon 2^+_1 excited state of ^{92}Zr (E=0.933 MeV, β_2 =0.13) and the single particle proton $1g_{9/2}$ state of ^{93}Nb. The contribution from direct processes to these levels was evaluated by the strong channel coupling method using the ECIS-79 computer program [33] and the optical potential parameters as in the case of the spherical optical model [32].

A comparison of the experimental data with calculational results shows a high quality for the data obtained for most levels. The slightly high cross section value for the E_j=949.99 keV, J^π=13/2$^+$ level points to the fact that the value of the spin for this level does not apper to be correct. However, as there were no other reasons to alter the spin of this level, its value was not changed in this analysis.

The evaluation of the energy spectra as well as of the angular and energy distributions in the continuum range, was based on the results of calculations performed at the Dresden Technical University (GDR) on the basis of the statistical approach to the multistep direct and compound nucleus processes [34]. Primary neutron emission spectra were subdivided according to the (n,n'γ), (n,2nγ) and (n,3nγ) processes, and secondary neutron

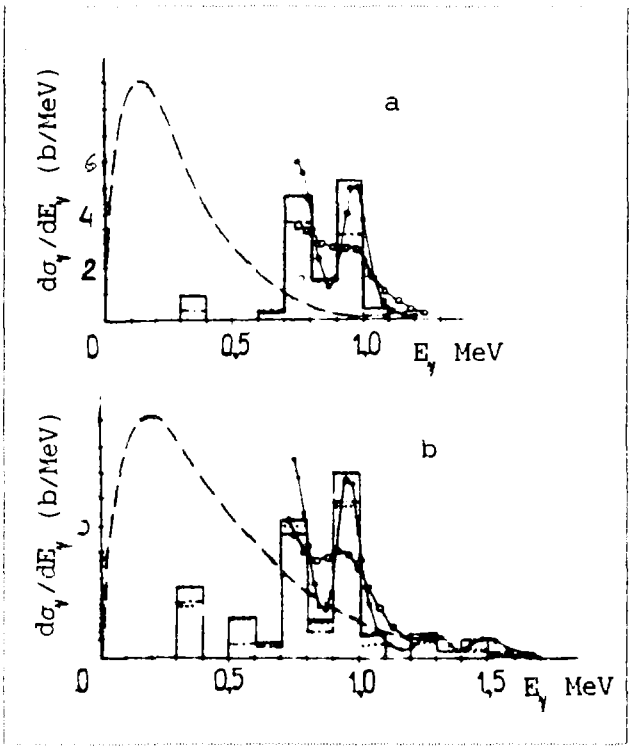

Fig.4. Gamma ray spectra from the inelastic scattering of neutrons on ^{93}Nb for neutron energies of 1.2 MeV (a) and 1.7 MeV (b). Results of this evaluation: (histogram) ——— , BROND [1] evaluation: — — — — . Experimental data: O [35], ● [36]. Calculated cross sections for the population of assumed discrete gamma lines summed over 100 keV energy ranges: —— · —— [21] and ··· [38].

emission spectra according to the (n,2nγ) and (n,3nγ) processes in compliance with the format and taking into account the values of the integral cross sections for each of these processes which were evaluated independently earlier. The resultant evaluated spectra complimented by the excitation functions of the discrete levels give a good description of the observed energy and angular distribution of secondary neutrons.

The gamma transition probabilities given in the Table below, and the evaluated level excitation functions allows one to evaluate the neutron inelastic scattering gamma ray spectra for neutron energies up to 1.8 MeV. Such an evaluation was performed and its results, together with the experimental spectrum data [35,36] and cross sections for the yield of discrete gamma rays [21,38], are shown in a spectral representation in Fig.4. It is evident that these spectra differ significantly from the temperature distributions which were widely used in earlier evaluations.

Level Scheme for Inelastic Scattering and Gamma Ray Transition Probabilities for ^{93}Nb

Level Number j	E_j in MeV	J^π	Gamma ray transition probability from level j to level k, I_k
0	0.0	$9/2^+$	ground level
1	0.0304	$1/2^-$	I = 1.0 metastable state
2	0.6868	$3/2^-$	$I_0 = 1.0$
3	0.744	$7/2^+$	$I_1 = 1.0$
4	0.8087	$5/2^+$	$I_0 = 1.0$
5	0.8101	$5/2^-$	$I_0 = 1.0$
6	0.9499	$13/2^+$	$I_1 = 1.0$
7	0.9791	$11/2^+$	$I_0 = 1.0$
8	1.0826	$9/2^+$	$I_0 = 0.34$, $I_3 = 0.66$
9	1.279	$3/2^-$	$I_0 = 1.0$
10	1.2974	$9/2^+$	$I_0 = 0.49$, $I_3 = 0.25$, $I_7 = 0.26$
11	1.3156	$5/2^-$	$I_0 = 0.81$, $I_4 = 0.19$
12	1.3351	$17/2^+$	$I_6 = 1.0$
13	1.3640	$1/2^+$	$I_5 = 1.0$
14	1.3952	$5/2^-$	$I_0 = 1.0$
15	1.4847	$3/2^+$	$I_0 = 0.81$, $I_4 = 0.19$
16	1.4914	$15/2^+$	$I_6 = 1.0$
17	1.5005	$7/2^+$	$I_0 = 1.0$
18	1.5700	$1/2^-$	$I_0 = 1.0$
19	1.6052	$9/2^+$	$I_0 = 0.17$, $I_6 = 0.57$, $I_7 = 0.19$, $I_8 = 0.07$
20	1.6649	$3/2^+$	$I_3 = 1.0$
21	1.6700	$9/2^+$	$I_0 = 0.19$, $I_3 = 0.50$, $I_{11} = 0.31$
22	1.6828	$11/2^+$	$I_0 = 0.28$, $I_3 = 0.48$, $I_7 = 0.24$
23	1.710	$5/2^+$	$I_0 = 1.0$

Experimental data given in reference [36] were used as the basis for the evaluation of the gamma ray spectra at neutron energies above 1.8 MeV. These spectra [36] were supplemented by soft gamma rays (E_γ < 0.75 MeV) whose magnitude were estimated on the basis of an analysis of all known experimental gamma ray yield data in this energy range. For the purpose of this analysis, the whole energy range from 0 to 0.75 MeV was subdivided into three ranges of 0.25 MeV each.

The evaluated gamma ray yield cross sections for each of these three energy ranges are shown in Fig.5 together with the corresponding experimental data which were obtained by integrating individual gamma ray spectra and by the summation of the yields of individual gamma lines in these energy ranges. The total gamma ray yield cross section which was determined by integrating gamma ray energy spectra over the whole energy interval is shown in Fig.6. The same figure shows the gamma ray yield cross section measured for E_γ> 0.75 MeV [36], as well as the evaluation given in reference [1]. As can be seen from these plots, the difference between the various evaluations is quite noticeable. In order to check the quality of the gamma ray spectrum evaluation, the average gamma ray energy yield from known gamma ray spectra was compared with the same quantity obtained from the evaluated level excitation cross sections and neutron inelastic scattering spectra. This comparison showed

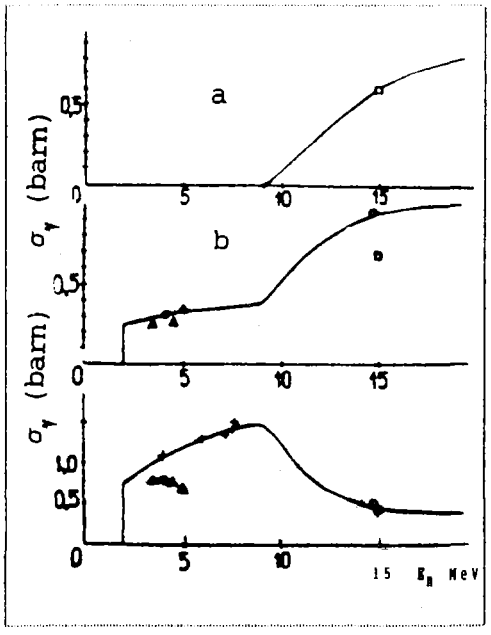

Fig.5. Gamma ray yield cross sections for (a) E_γ = 0 to 0.25 MeV, (b) E_γ = 0.25 to 0.50 MeV and (c) E_γ = 0.50 to 0.75 MeV for the interaction of neutrons with ^{93}Nb. Results of this evaluation: ———; experimental data: ▲ [38], ● [39], □ [40], + [41], and O [42].

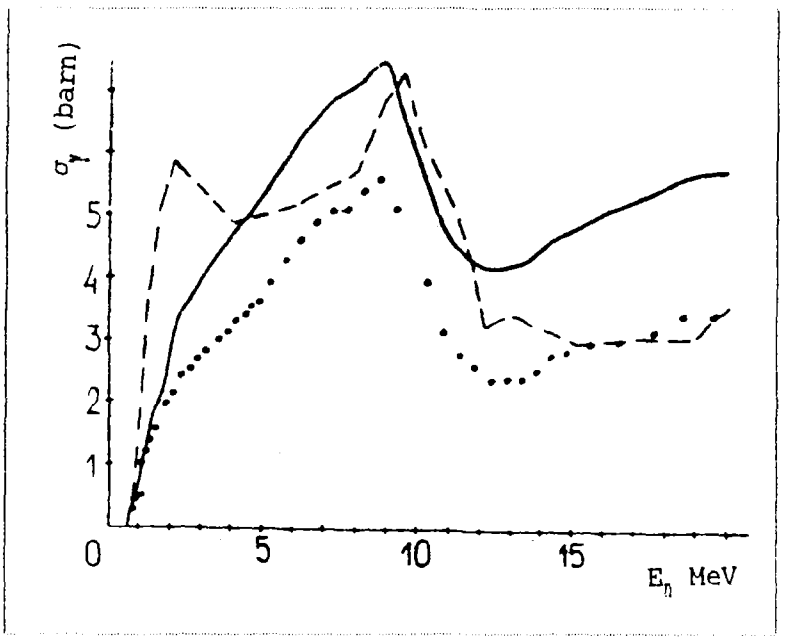

Fig. 6.Total neutron induced gamma ray yield cross section for ^{93}Nb. Results of this evaluation: ——— ; BROND [1]: ——·——·—— ; ● integrated gamma ray spectra for energies E_γ > 0.75 MeV based on an assumed isotropic gamma ray angular distribution and on measurements taken at 125° as reported in reference [36].

that the two quantities agree to within 10%, at least up to the (n,2n) reaction threshold.

The authors are hopeful that the results of this re-evaluation of the BROND evaluation of ^{93}Nb will be used in the nuclear analysis of fusion reactors.

REFERENCES

[1] USSR NUCLEAR DATA CENTER, Recommended Evaluated Neutron Data Library BROND (MANOKHIN, V.N., Ed.), Obninsk, USSR (1986).

[2] Nuclear Data Sheets 88 (1972) 527.

[3] BROWNE, E., DAIRIKI, J.M., DOEBLER, R.E., Table of Isotopes, 7th Edition, (LEDERER, C.M., SHIRLEY, V.S., Eds.), Wiley, New York (1978).

[4] COLES, R.E., Rep. AWRE-O-66/71 (1971).

[5] SMITH, A.B., GUENTER, R.T., WHALEN, J.F., Z.Physik 264 (1973) 39.

[6] REITMAN, D., ENGLEBRECHT, C.A., SMITH, A.B., Nucl.Phys. 48 (1963) 593.

[7] SMITH, A.B., GUENTER, R.T., WHALEN, J.F., Z.Physik 264 (1973) 39.

[8] ALMEN-RAMSTROM, E., Rep. AE-503 (1975).

[9] THOMPSON, D.B., Phys.Rev. 129 (1963) 1649.

[10] HOPKINS,J.C., DRAKE, D.M., Nucl. Sci. and Eng. 36 (1969) 275.

[11] BIRYUKOV, N.S., ZHURAVLEV, B.B., KORNILOV, N.V., Yadernaya Fizika 19 (1974) 1201 (in Russian).

[12] SIMAKOV, S.P., LOVCHIKOVA, G.N., LUNEV, V.P., Yadernaya Fizika 37 (1983) 801 (in Russian).

[13] GOEBEL, H., FEICHT, E.J., VONACH, H., Z.Physiz 240 (1970) 430.

[14] KOZYR, Yu.E., PLUZHKO, V.A., PROKOPETS, G.A., Proc. International Conference on Neutron Physics, USSR, 2 (1977) 52 (in Russian).

[15] HERMSDORF, D., SASSONOFF, S., SEELIGER, D., et al., Rep. ZfK-262 (1973) 28.

[16] NATH, N., ROTHMAN, M.A., VAN-PATTER, D.M., et al., Nucl.Phys. 14 (1959) 78.

[17] ROTHMAN, M.A., VAN-PATTER, D.M., DUBEY, V.S., et al., Phys. Rev. 107 (1957) 155.

[18] BRODER, D.L., KOLESSOV, V.E., LASHUK, A.I., et al., Atom. Energh. 16 (1964) 103.

[19] LEGTYAREV, Yu.G., PROTOPOPOV, V.N., Izv.Akad.Nauk USSR, Ser. Fizika 35 (1971) 2341 (in Russian).

[20] VAN HEERDEN, I.J., McMURRAY, W.R., SAAYMAN, R., Z. Physik 260 (1973) 9.

[21] ROGERS, V.C., BEGHAIN, L.E., et al., Nucl. Sci and Eng. (1971) 297.

[22] NEMILOV, Yu.A., KRAMAROWSKI, Ya.M., TETERIN, E.D., et al., Problems of Atomic Science and Technology. Ser. Nuclear Constants 3 (1986) 25 (in Russian).

[23] HINO, Y., YAMOMOTO, T., ITAGAKI, S. et al., Proc. International Conference on Nuclear Data for Technology, Knoxville, TE, (1979) 408.

[24] WALT, M., BARSHALL, H.H., Phys. Rev. 93 (1954) 1062.

[25] GLASKOV, N.P., Atomnaya Energiya 14 (1963) 400 and 416 (in Russian).

[26] ABRAMOV, A.I., Atomnaya Energiya 12 (1962) 62 (in Russian).

[27] HORSLEY, A., Nucl. Data 2A 3 (1965) 243.

[28] KINNEY, W.E., PEREY, F.G., Nucl. Sci. and Eng. 63 (1977) 418.

[29] MOLDAUER, P.A., in Proc. IAEA Workshop on Nuclear Model Computer Codes, Trieste, Italy, 1984.

[30] JAPANESE NUCLEAR DATA CENTER, Japanese Evaluated Nuclear Data Library, JENDL-2, Rep. JAERI-M-84-103 (1984) Mat.# 2411.

[31] GILBERT, A., CAMERON, A.G.W., Can. J. Phys. 43 (1965) 1446.

[32] SMITH, A.B., GUENTER, P.T., LAWTOR, R.D., Rep. ANL-INDM-91 (1985).

[33] RAYNAL, J., in Proc. IAEA Workshop on Nuclear Model Computer Codes, Trieste, Italy, 1984.

[34] HALKE, H., SEELIGER, D., ZHIVOPIVTSEV, F.A., Z. Physik A239 (1988) 331.

[35] MORGAN, G.L., PEREY, F.G., Rep. ORNL-TM-5829 (1977).

[36] DICKENS, J.K., MORGAN, G.L., NEWMAN, E., Rep. ORNL-TM-4972 (1975).

[37] SANTRY, A., Rep. PRCMA-27 (1974) 14.

[38] WILLIAMS, G.H., Rep. ORO-2791-30 (1969) 141.

[39] MATHUR, S.C., BUCHANAN, P.S., MORGAN, I.L., Bull. Am. Phys. Soc. 12 (1967) 921.

[40] ZHOU HONDU, TANG ZIN, YAN YIMING, et al., IAEA Rep. INDC(CPR)-10 (1986).

[41] DRAKE, D.M., HOPKINS J.C., YOUNG, O.S., et al., Nucl. Sci. and Eng. 40 (1970) 294.

[42] DRAKE, D.M., ARTHUR, E.D., SILBERT, M.G., Nucl. Sci and Eng. 65 (1978) 49.

ISOTOPIC DEPENDENCE OF THE RADIATIVE CAPTURE CROSS-SECTION FOR MEDIUM AND HEAVY MASS NUCLEI AT NEUTRON ENRGIES RANGING FROM 0.5 TO 2.0 MeV

Yu.N. Trofimov

Abstract

A simple formula to estimate the radiative capture cross-section as a function of the relative neutron excess has been derived. The calculated results are compared with existing measured and evaluated cross-section values. Neutron capture cross-sections for important fission product isotopes were evaluated at energies between 0.5 and 2.0 MeV.

The demand for nuclear data in the vigorously developing area of nuclear power is growing continuously. Accurate and reliable neutron data are needed for the numerical analysis of fast neutron reactors. By and large, the requirements for microscopic (n,γ) reaction cross sections are not satisfied, either because of the complete absence of the required data, contradictions in the existing experimental data, or because of the poor accuracy of the neutron radiative capture (P3) cross-sections. The accuracy requirement of P3 neutron cross sections is as follows: 10% for the (^{237}Np and ^{236}U) fuel cycle, 5% for the Cd, Eu, Gd, Er and Hf neutron absorbers, 10% for Fe, Mo, and Mn components of construction materials, and 10% for the fission products. In view of the difficulties in the measurement of these data in the 0.5 to 2.0 MeV energy range a significant increase in the availability of these data cannot be expected. Experimental data for the P3 reaction cross-sections in this neutron energy range are completely absent for 120 of the 200 medium and heavy stable isotopes, including the following isotopes important for reactor development: $^{50,52-54}$Cr, $^{54,56-58}$Fe, $^{58,60-62}$Ni, ^{95,97,100}Mo, ^{101,102,104}Ru, ^{105}Pd, ^{131}Xe, ^{133}Cs, ^{141}Pr, ^{143,145}Nd, ^{149}Sm and ^{153}Eu.

Evaluated P3 reaction data for the radioactive Po, At, Rn, Fr, Ra, Ac, Am, Cm, and Cf elements are completely absent, and there is a dire need for an improvement in the evaluations of the fission product P3 neutron reaction cross-sections.

The evaluation of the isotopic P3 neutron reaction cross-sections is usually performed using the statistical theory of nuclear reactions complemented by the optical model potentials. In this connection it is essential to know the optimum values of the following parameters: level densities (there are very few nuclei for which spins and level densities are known completely and exactly), optical potential parameters, neutron and radiation strength functions for various l, and the potential scattering radius. The evaluation of the P3 neutron reaction cross-section in the 1-2 MeV energy range is basically qualitative. At 14 MeV, evaluated values of the P3 cross-sections using statistical theory of nuclear reactions are already a few orders of magnitude lower than experimental data. The uncertainty of such evaluations is approximately 50% [1]. If one considers the large number of approximations and assumptions made in the model, the evaluation of the uncertainty is to a large extent subjective, and its values are underestimated and difficult to substantiate. Calculated values of cross-sections cannot replace measurements. However, even at the present time it is impossible to measure the neutron induced P3 reaction cross-sections of actinides, fission products, numerous radioactive nuclei, as well as isotopes which are not abundant in nature. The radiative capture reaction in many stable isotopes result in stable reaction products and can therefore not be investigated by the highly sensitive activation method. The use of other methods (e.g. transmission method, large scintillation tank method, etc.) requires considerably larger isotope sample sizes (10 to 100 g) which are difficult to achieve by enrichment.

The generally accepted method to represent experimental and evaluated P3 cross-section data for individual isotopes is in the form of an energy dependent representation of $\sigma(E_n)$. It seems to us, however, that it would be more informative to represent the neutron induced P3 cross-section as a function of the isotopic mass number, namely $\sigma(A)$. In this exercise it is proposed to perform the evaluation of the neutron induced P3 cross sections of medium and heavy nuclei solely on the basis of the number of neutrons and protons in the nucleus, without resorting to nuclear model representation parameters. The only input used are values of the P3 cross-sections for not more than one isotope of the investigated element.

The result of the analysis of our data and of the published data showed that the value of neutron induced P3 cross-sections of stable isotopes of a given element decreases as the atomic weight of the nuclide increases. In order to confirm this behavior we performed additional activation measurements of the P3 reaction cross-section for the following 48 stable isotopes in the neutron energy range of 0.5 to 2.2 MeV: ^{55}Mn, ^{58}Fe, ^{68}Zn, ^{71}Ga, ^{74}Ge, ^{82}Se, ^{84}Sr, ^{96}Zr, ^{98,100}Mo, ^{102,104}Ru, ^{106,110,114,116}Cd, ^{113}In, ^{116,122}Sn, ^{121,123}Sb, ^{139}La, ^{140,142}Ce, ^{146,148,150}Nd, ^{151}Eu, ^{152,154}Sm, ^{158}Gd, ^{164}Dy, ^{162,164,170}Er, ^{175}Lu, ^{176}Yb, ^{179,180}Hf, ^{185,187}Re, ^{186}W, ^{190,192}Os, ^{191,193}Ir, ^{236}U, ^{237}Np.

The following conclusions can be made on the basis of these results:

1. The neutron induced P3 cross-section is a function of the excess of neutrons with respect to the protons in the nucleus. As the number of "surplus" (excess) neutrons in the target nucleus increases, the cross-section value decreases. The following isotopic dependence can be formulated on the basis of the evaluation of the neutron induced P3 cross-sections:

$$\sigma_\alpha = \sigma_0 \, e^{-k\alpha} \qquad (1)$$

where σ is the P3 neutron cross-section, $\alpha = (N-Z)/A$ is the parameter for the relative neutron excess value, k is a constant, and N and Z are the number of neutrons and protons in the nucleus respectively.

2. The P3 cross-section is a function of the parity of neutrons or protons in the target nucleus. Equation (1) was not made more complex by introducing the correction to take the nucleon parity into account. Instead, the whole complex of nuclei considered in this exercise was subdivided according to parity into four groups: 1) even-even, 2) odd-even, 3) even-odd and 4) odd-odd nuclei. The fourth group was devoid of stable medium and heavy mass nuclei. Let us now analyze the nuclear data situation for each of the four groups.

Even-even nuclei. The investgation of the neutron induced P3 cross-sections of even-even nuclei revealed the fortuitous fact that among the isotopes of any given element, those isotopes

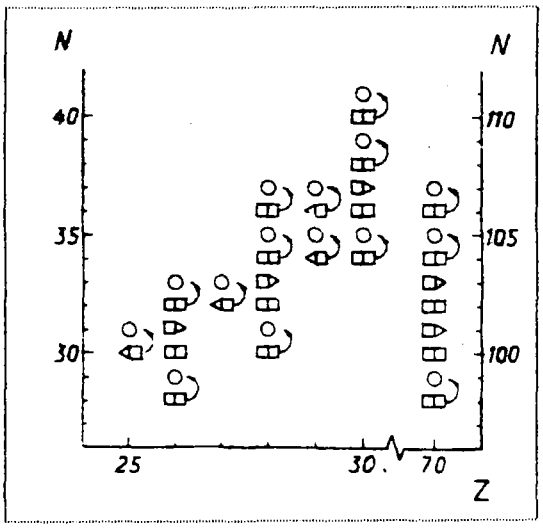

Fig. 1. Part of the table of isotopes showing medium mass nuclei. Designation of stable nuclei: even-even nuclei, odd-even nuclei, even-odd nuclei.

The arrows indicate (n,γ) reactions with the formation of radioactive reaction products (0).

having a minimal and maximal mass number are always even, and that the (n,γ) reaction products of these isotopes are always radioactive. This can be seen very well in Fig. 1 which reproduces that part of the table of isotopes which covers medium mass nuclei. The arrows show (n,γ) reactions with the formation of radioactive reaction products. It is therefore possible to measure the neutron induced P3 cross-section of at least two isotopes of each even Z element using the activation method, providing that these measurements do not present significant dificulties (such as a very short half-life, inadequate gamma ray yield, etc.). For many even-even nuclei, however, the end product of an (n,γ) reaction is a stable nuclide which precludes the use of the activation method. The experimental investigation of such nuclei by other methods is difficult because of the extreme enrichment requirement. (In addition, it must be noted that many odd Z elements are monoisotopic).

Odd-even nuclei. Elements which comprise this group of nuclei have either one or two stable isotopes. The neutron induced P3 cross-sections of isotopes of this group have been measured successfully because the end product of the (n,γ) reaction is always in a radioactive state, and the activation method is applicable in all cases.

Even-odd nuclei. Among all of the 45 stable isotopes of this group, there is not one isotope which can produce a radioactive reaction product as a result of a neutron induced P3 reaction. The activation method is therefore not applicable for

this group of nuclei. There are very few (n,γ) reaction cross-sections which have been measured by means other than activation.

DERIVATION OF EQUATION (1)

Ericson, Cusocrea and other authors [2] have used the following relationship, derived on the basis of the evaporation approximation of the statistical model, to calculate (n,p) reaction cross-sections:

$$\sigma = k_1 . \sigma_o . e^{k_2(Q - k_3 B)}, \ldots\ldots\ldots, \qquad (2)$$

where σ, Q are the reaction cross-section and energy,
σ_0 is the geometrical nuclear cross-section,
B is the Coulomb barrier of the nucleus, and
k_{1-3} are constants.

Applying equation (2) to the evaluation of the (n,γ) reaction cross-section, we obtain

$$\sigma = k_1 . \sigma_o . e^{k_2 S_n}, \ldots\ldots\ldots\ldots\ldots, \qquad (3)$$

where S_n is the binding energy of the neutron to the target nucleus (or the separation energy of the neutron from the compound nucleus)

For most stable and radioactive isotopes, the parameter S_n is approximately linearly dependent on the relative neutron excess represented by the parameter α. Figs. 2 a and b show the dependence of the neutron binding energy on the α parameter for even-even and even-odd nuclei. The values for the S_n parameter have been taken from references [3] and [4]. The continuous lines connect the energy values for nuclei having the same Z. As a rule, the curves are smooth, decreasing monotonically with increasing α, almost linearly for nuclei from any of the four parity groups with the exception of magic number nuclei and in regions where there is a change in the shape of the nucleus. In these regions there is a change in the slope of the $S_n(\alpha)$ curve. Deep depressions of the neutron binding energy correspond to nuclei having a magic number of neutrons (N=50,82,126). The monotonically decreasing behavior is also disrupted in the regions of transition from spherical to deformed nuclei (N=90) and from deformed to spherical nuclei (N=114). In the region of

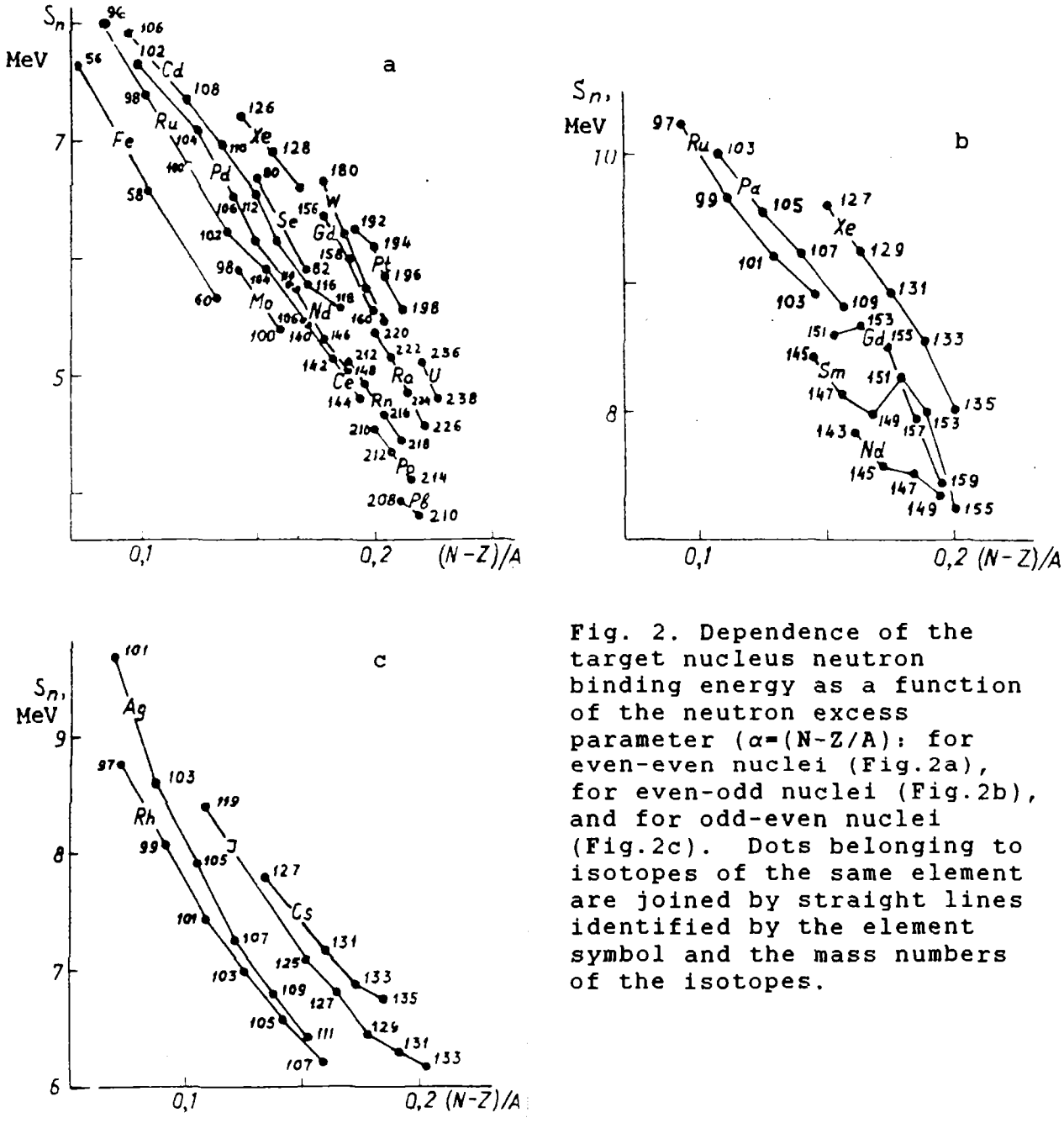

Fig. 2. Dependence of the target nucleus neutron binding energy as a function of the neutron excess parameter (α=(N-Z/A): for even-even nuclei (Fig.2a), for even-odd nuclei (Fig.2b), and for odd-even nuclei (Fig.2c). Dots belonging to isotopes of the same element are joined by straight lines identified by the element symbol and the mass numbers of the isotopes.

N=90,92, the binding energy does not only remain constant as α increases, but it increases with respect to the S_n values of neighboring nuclei. The monotonically decreasing behavior of $S_n(\alpha)$ resumes as α increases (see Fig.2b, Sm).

Taking the linear dependence of S_n on α into consideration, equation (3) is reduced to

$$\sigma_\alpha = \sigma_0 \cdot e^{k\alpha} \ldots\ldots\ldots\ldots,$$

where σ_α and σ_0 are the isotopic neutron induced P3 cross-sections for the neutron excess parameter α and for α=0 (i.e.N=Z), respectively.

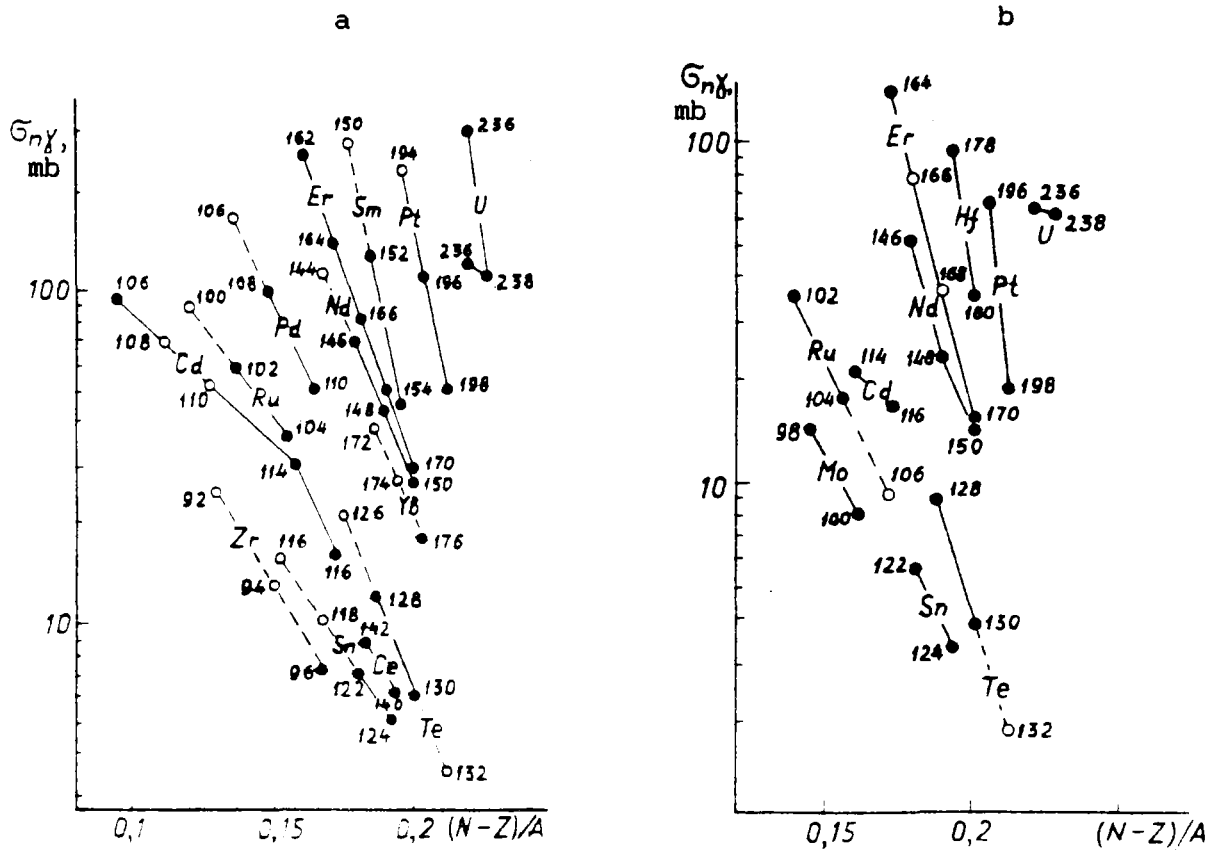

Fig. 3. Dependence of the neutron-induced P3 cross-section on the neutron excess parameter: a) for even-even nuclei, E_n=0.5 MeV, b) for even-even nuclei, E_n=2.0 MeV, c) for odd-even nuclei, E_n=0.5 MeV.

Data: measured ● and evaluated O results by author for this work. The recommended isotopic dependence $\ln\sigma_{n\gamma}(\alpha)$ is given by the dotted lines.

The dependence on the neutron excess parameter of the natural log of the P3 cross-section for the isotopes of a given element at a given neutron energy should therefore be approximately linear. Note that an analogous systematic behavior for (n,p) and (n,α) reactions at 14 MeV was derived by Levkovskij [5]. Figs.3 a, b and c show the author's experimental results of his current work [6] and data from reference [7] on (n,γ) reaction cross-sections for even-even nuclei at 0.5 and 2.0 MeV, and for odd-even nuclei at 0,5 MeV. The figures als show evaluated values of the P3 cross-sections, represented by dotted lines for those isotopes for which there are no measured data. Figures 2 and 3 show a distinct correlation of the dependence of S_n and $\ln\sigma_\alpha$ on α. The only exception to this general rule represented by equation (1), is the P3 cross-section for ^{236}U. Two different sets of data exist for this nuclide: the soviet results given in references [8,9], and the western results published in references [10,11], where the results of the latter are twice as high as the former. Taking the reliability of the neutron-induced P3 cross-section for ^{238}U into consideration, one must admit that the western data agree better with equation (1). It can be seen that the P3 cross-sections for isotopes of a given element are intimately related to each other. Thus, measured or evaluated neutron-induced P3 cross-sections for one isotope automatically determine the values of P3 cross-sections for the other isotopes with the exception of magic nuclei, and of those nuclei which are undergoing a shape change. A large variation in the values of the neutron induced P3 cross-sections can be observed in those nuclei which have the same number of protons and neutrons (N=Z). As the number of neutrons in the nucleus increases, this diversity disappears, and the P3 cross-sections of neutron rich nuclei assume smaller values which fall within the average for the elements; it is as if they give up their individuality.

The isotopic dependence of the neutron induced P3 cross-section gives us the possibility to use it in order to:

- eliminate contradictory or suspicious results;
- check new experimental data;
- predict the cross-sections of nuclei which are difficult to measure (e.g., stable reaction products, small cross

section values, interfering competing reactions, small gamma ray yield, etc...); and to

- predict neutron induced P3 cross-sections of radioactive target isotopes.

The isotopic dependence is also of interest in the formulation of nuclear models. One of the advantages of this isotopic dependence is that the prediction of neutron induced P3 cross-sections does not depend on the knowledge of nuclear level schemes, level densities or radiation widths. At the same time this isotopic dependence can also be used in selecting reactor materials. Reactor materials are not only chosen on the basis of their mechanical, thermal and chemical properties, but also on the nuclear characteristics of the component isotopes. Thus, materials with a high P3 neutron absorption capacity must be chosen among neutron deficient nuclei (particularly odd Z nuclei in the rare earth element group). Using the isotopic dependence represented by equation (1), it is very easy to calculate the P3 cross-section of an element having a natural isotopic composition, knowing the P3 cross-section for only one of the stable (or radioactive!) component isotopes.

APPLICATION OF THE ISOTOPIC DEPENDENCE EQUATION (1) IN THE EVALUATION OF FAST NEUTRON P3 CROSS-SECTIONS OF THE MOST IMPORTANT FISSION PRODUCT NUCLEI

It is of extreme interest to know the evaluated values of the neutron induced P3 cross-sections of the radioactive ^{238}U fission products, for which there are no experimental data, in order to estimate their contribution to the total neutron absorption in the core of a fast reactors.

As an example, let us apply the isotopic dependence to the evaluation of the neutron induced P3 cross-section for the following nuclei $^{95,97}Nb$, ^{105}Rh, ^{106}Ru, ^{111}Ag, $^{129,131}I$, ^{132}Te, ^{135}Cs and ^{141}Ce. The evaluated values of the neutron induced P3 cross-sections for these nuclei, as well as the reference (n,γ) reaction cross-sections for the stable isotopes of those elements are given in the Table below. Comparisons of the cross-sections calculated using equation (1) (represented by dots) with evaluated values given in ENDF/B-V (dotted curve), JENDL-1

Calculated neutron radiative capture cross-sections of radioactive nuclei using equation (1), and reference (n,γ) reaction cross-sections of stable isotopes.

E_n	Reference Isotope					Evaluated Isotope			
MeV	Symbol, $\sigma(n,\gamma)$ mb				Ref.	Symbol, eval. $\sigma(n,\gamma)$ mb			
0.5	Nb93	60			[7]	Nb95	39	Nb97	26
1.0		30					20		13
1.5		13					9		6
0.5	Rh103	130			[7]	Rh105	78		
1.0		70					45		
2.0		50					32		
0.5	Ru102	42	Ru104	36	Our	Ru106	24		
1.0		53		27	Data		14		
1.5		25		18	[6]		11.5		
2.0		35		15			8		
0.5	Ag107	177	Ag109	110	[7,12]	Ag111	69		
1.0		110		70			44		
1.5		104		59			33		
2.0		100		50			24		
0.5	I127	120			[7.13]	I129	62	I131	33
1.0		72					58		44
1.5		55					40		26
2.0		50					37		28
0.5	Te128	12	Te130	6	[7,14]	Te132	3.6		
1.0		10		4.5			2.4		
1.5		9		4			2		
2.0		8		3.5			1.7		
0.5	Cs133	120			[7,15]	Cs135	57		
0.5	Ce142	8.5			Our	Ce144	6		
1.0		6.4			Data		5		
1.5		6.5			[6]		4.5		
2.0		5.9					3.6		

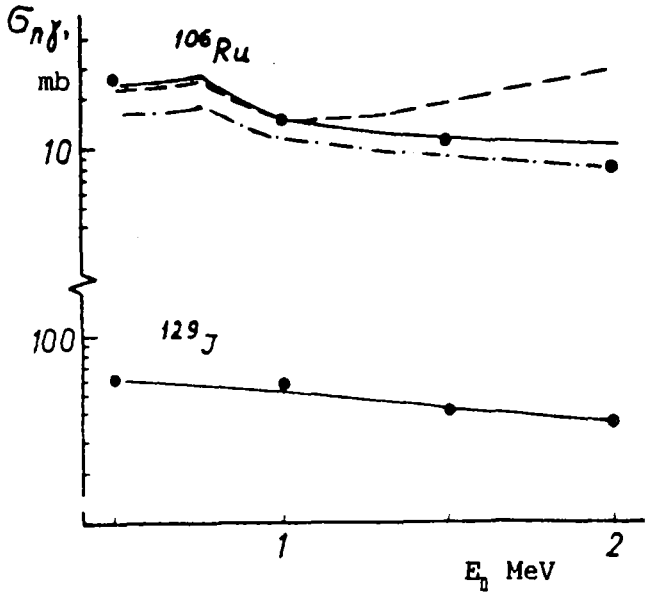

Fig. 4a. Comparison of the neutron induced P3 cross-sections of the ^{106}Ru and the ^{129}I isotopes.

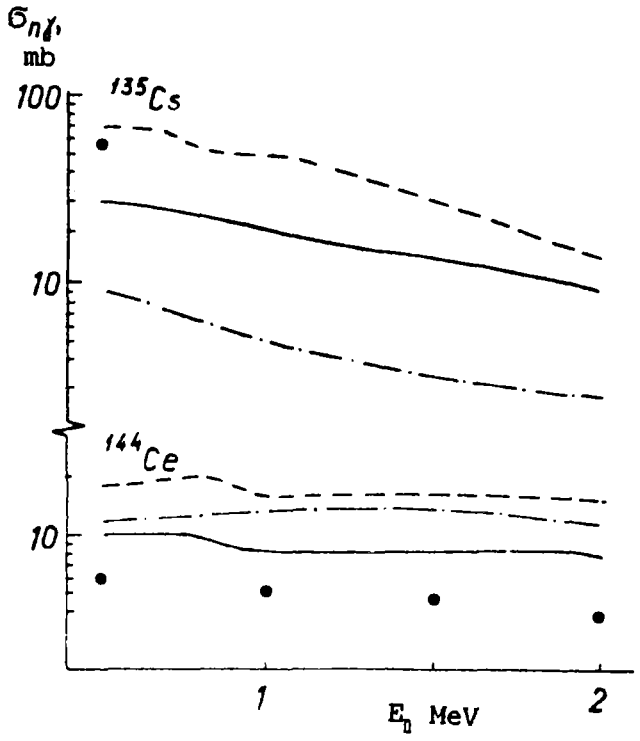

Fig. 4b. Same caption as for Fig. 4a but for the isotopes ^{135}Cs and ^{144}Ce.

ENDF/B-V - - - - - - -
JENDL-1 — · — · — · —
FEI [16] ————————
Author's results ●

(point-dot curve) and FEI [16] (continuous curve) are given in Figs. 4a and b. Our evaluation agrees with the FEI evaluation for ^{106}Ru and ^{129}I; although our evaluation of ^{144}Ce is 30% lower then the FEI evaluation, it disagrees even more with the other evaluations. The shape of the curve, however, is well reproduced. Our evaluated value of the ^{135}Cs P3 cross-section at 0.5 Mev is 57 mb, which is approximately twice as large as the FEI evaluated value, but is in agreement with the ENSDF/B-V evaluation.

The uncertainties of the evaluated data were determined individually and depend on the uncertainty evaluation method. In its logarithmic form, the isotopic dependence equation (1) is linear:

$$\ln\sigma_\alpha = \ln_0 - k\alpha \qquad (4)$$

where $\ln_0$ and k are constants.

The evaluation of the cross-section or the positioning of the straight line given by equation (4) in the $\ln\alpha$ and α coordinate space can be determined by two methods:

1. By knowing the values of the P3 cross-sections for two isotopes. If the uncertainties of the reference isotope cross-sections are known to 10%, then the uncertainty of the neighboring isotope which is being investigated will have the same uncertainty.

2. By knowing the cross-section value for one reference isotope and the slope of the line given by equation (4), which can be determined by analogy to the slope of the neighboring nuclei (as a function of Z and corresponding to the same parity group). For this method, the assigned uncertainty was 20-30 %.

REFERENCES

[1] STAVISKIJ, Yu.Ya., ABRAMOV, A.I., VAN'KOV, A.A., et al., Fast neutron radiative capture, Moscow, Atomizdat (1970) (in Russian).

[2] TROFIMOV, Yu.N., Problems of Atomic Science and Technology. Ser. Nuclear Constants 2 (1979) 47 (in Russian).

[3] KRAVTSOV, V.A., Atomic masses and binding energies of nuclei, Moscow, Atomizdat (1974) (in Russian).

[4] BYCHKOV, V.M., GRUDZEVICH, O.T., PLYASKIN, V.I., Problems of Atomic Science and Technology. Ser. Nuclear Data 3 (1987) 14 (in Russian).

[5] LEVKOVSKIJ, V.N., JETP 2 8 (1963) 305 (in Russian).

[6] TROFIMOV, Yu.N., Problems of Atomic Science and Technology. Ser. Nuclear Constants 4 (1987) 10 (in Russian).

[7] BELANOVA, T.S., IGNATYUK, A.V., PASHCHENKO, A.B., PLYASKIN, V.I., Neutron radiative capture, Moscow, Energoatomizdat (1986) (in Russian).

[8] TOLSTIKOV, V.A., Problems of Atomic Science and Technology. Ser. Nuclear Constants 4 (1986) 23 (in Russian).

[9] TROFIMOV, Yu.N., Atomnaya Energiya 64 2 (1988) 150 (in Russian).

[10] BARRY, J.F., BUNCE, J.L., PERKIN, J.L., Proc.Phys.Soc. 78 503 (1961) 801.

[11] STUPEGIA, D.C., HEINRICH, R.R., MacLoud, I.H., J.Nucl.Energy A/B 15 (1961) 200.

[12] MACKLIN, R.L., Nucl.Sci. and Eng. 82 (1982) 400.

[13] STAVISKIJ, Yu.Ya., Atomnaya Energiya 10 (1961) 158 (in Russian).

[14] LOVBENKO, A.G., KOLESSOV, V.E., KOROLEVA, V.P., et al., Atomnaya Energiya 25 (1968) 529 (in Russian).

[15] MACKLIN, R.L., Nucl.Sci. and Eng. 81 (1982) 418.

[16] IGNATYUK, A.V., KRAVCHENKO, I.V., MANTUROV, G.N., Problems of Atomic Science and Technology. Ser. Nuclear Constants 1 (1987) 3 (in Russian).

EXPERIMENTAL DETERMINATION OF THE $^{27}Al(n,\alpha)^{24}Na$ REACTION CROSS-SECTION FOR 14.8 MeV NEUTRONS *

N.N. Moisseev, Z.A. Ramendik, V.T. Shchebolev

Abstract

The $^{27}Al(n,\alpha)^{24}Na$ reaction cross-section was measured by the activation method for 14.8 MeV neutrons. The measured value of this cross-section was 110±2 mb. The neutron flux was determined to an accuracy of less than 1%. Measurement of the induced activity was carried out by beta-gamma coincidence and by gamma spectrometry.

The $^{27}Al(n,\alpha)^{24}Na$ cross-section is widely used as a standard in the relative measurement of neutron reaction cross-sections as well as in precision measurements of the neutron flux at neutron energies ranging from 13 to 16 MeV on neutron generators and accelerators [1,2]. Incidentally, the collection of threshold activation detectors made of aluminium at the National Physical Laboratory in the U.K., standardized to a number of nuclides and equipped with recommended cross sections is used as the secondary standard in neutron flux density measurements [2].

Achievements in neutron metrology and in the measurement of radionuclide activities have allowed the performance of precision experiments to determine the cross-section of this reaction to a high degree of accuracy which is estimated by the authors to be in the range of 2% to 5 %. However, the differences in the values of this cross-section exceed the bounds of the assigned uncertainties which, according to existing data compilations [3], can be as high as 10% to 15%.

The exercise described on this report is part of a general programme designed to determine precise values of activation reaction cross-sections induced by 14.8 MeV neutrons. The samples consisted of particularly pure aluminium machined in the form of discs having a diameter of 30 mm and a thickness of 0.5 to 1.0 mm. The number of atoms in each sample was determined

* This report was presented at the 1st International Conference on Neutron Physics, held in Kiev, on 21-25 September, 1987.

from results of very exact weighing, and chemical and mass spectrometric analysis. The samples were positioned parallel to the surface of the neutron generator target located at a distance of 83.3 mm and at an angle of 10° to the direction of the ion beam. The neutrons were generated by the $T(d,n)^4He$ reaction. Under the given conditions, the neutron energy determined by the slowing down of the ion beam in the target and by the geometry factor, was 14.79 MeV with an uncertainty ranging from $-\Delta E=0.08$ MeV and $+\Delta=0.22$ MeV. Each sample was irradiated for 3 to 5 hours with a continuous monitoring of the neutron flux at 100 s intervals. The neutron flux (whose magnitude was on the order of 10^6 per cm^2 per s) was measured for each irradiation period using three independent methods [4]: by the scintillation method using the hydrogen scattering cross-section as the standard, by measuring the counting rate of accompanying particles and by detecting neutron helium coincidences.

The calculated neutron flux density was corrected for the monitor counting rate (taking the decay rate into account) which permitted the exclusion of small variations in the neutron field caused by the fluctuation of the ion beam current and the accelerating voltage of the generator.

The irradiated samples were allowed to decay for 0.5 to 3 hours in order to minimize the effect of the activity induced by the $^{27}Mg(n,p)$ reaction whose reaction product decays with a half-life of 9.5 min. The induced activity was measured by two methods: using a NaI(Tl) scintillation spectrometer and the AMA 02-F1 automated multichannel analyzer and a low background beta-gamma coincidence detector [5]. In order to increase the reliability and accuracy of the activity measurements, the detection and metrological instrumentation were standardized using the governmental primary activity calibration standards [6]. A new set of (OSGI-3-2) standard spectrometrical gamma ray source samples, certified to an accuracy of 1.5% (with a confidence level of 0.99) were also used for this purpose.

The measured spectra were processed with the use of a computer program which performed smoothing of the data, subtraction of the background approximated by the quadratic function, calculation of

the total absorption peak by means of the least squares method and the calculation of the areas under the peaks. Using the ^{228}Th sample provided with the OSGI-3 source standardization set, it was possible to extend the detection efficiency curve of the spectrometer up to an energy of 2.7 MeV, which allowed us to measure the activity of both the 1.3686 MeV and the 2.7540 MeV lines of the ^{24}Na. radionuclide.

During the analysis of the 1.369 MeV peak it became apparent that for samples counted for more than one hour, the right side of the 1.369 MeV peak exhibited a distortion. With the aid of subsequent experiments it was determined that this effect was due to the radiation emitted by the 1.469 MeV line of the ^{40}K nuclide contained in structural parts of the spectrometer and of the room. After the elimination of this effect, the results of the measurements of the 1.369 MeV line for various detection times showed a much better aggreement. The effect of the self-absorption in the aluminium samples was also investigated by putting the standard reference source samples of the OSGI set between aluminium foils of different thickness. The results of this experiment were in good aggreement with calculated values using absorption coefficients for gamma rays in aluminium.

The beta-gamma coincidence detector has the advantage of yielding absolute values of nuclide activities. Because of the relatively low activity level induced in the irradiated ^{24}Na samples, the main source of error arising in coincidence method measurements was the background in the beta channel, and a background due to spurious coincidences. The self-absorption effect correction was not applied to the coincidence measurements (it was estimated that the contribution of this effect to the overall uncertainty was less than 1.0%).

In total, ten sample irradiation cycles and twenty induced activity measurement series were performed. The reaction cross section values obtained by the scintillation method and by the coincidence method were calculated separately. The cross-section values and the origin of the errors and their values, for the two methods are given in the Table below.

Measurement Method Characteristics

Method	Source of error	Error %	Cross-Section Value
Scintillation gamma spectrometer with NaI(Tl) crystal	Determination of neutron flux density	1.0	110.2 mb $\Delta_{0.95}$=2.4%
	Detection efficiency	1.5	
	Self-absrption in sample	0.2	
	Geometry factor	0.2	
	Photo peak area	0.5	
	Correction of half-life	0.1	
	Time interval measurement	0.1	
	Number of atoms in sample	0.05	
Beta-gamma coincidence method	Determination of neutron flux density	1.0	109.8 mb $\Delta_{0.95}$=2.1%
	Activity measurement	1.0	
	Background count rate correction	0.5	
	Undetermined self-absorption	1.0	
	Correction of half-life	0.1	
	Time interval measurements	0.1	
	Number of atoms in sample	0.05	
	Random error	0.3	

The results obtained in this manner were in good agreement with each other. The combined relative uncertainties, calculated in accordance with the methodology prescribed in GOST 8.207-76 [7], are given to a confidence level of 0.95. The final value of the $Al(n,\alpha)^{24}Na$ reaction cross-section for 14.8 MeV neutrons, obtained by taking the weighted average of the measured values is:

$$\sigma = 110 \pm 2 \text{ mb}$$

This result is in good agreement with the evaluated value of 112.3 mb given by the IAEA in 1983 [8] for the energy range of 14.75 MeV to 14.85 MeV.

REFERENCES

[1] AXTON, E., Proc. Symposium on Neutron Monitoring for Radiation Protection Purposes, IAEA, Vienna, Vol.2 (1977) 431.

[2] ROBERTSON, J., et al., Nuclear Energy 27 (1973) 531.

[3] SHETT, A., OKAMOTO, K., Compilation of threshold reaction neutron cross-sections for neutron dosimetry and other applications, EANDC 95 "U", Centre de Compilations de Donnees Neutroniques, Gif-sur-Yvette (1974).

[4] SHCHEBOLEV, V.T., RAMENDIK, Z.A., Proc. Fifth All-Union Conference on Neutron Physics, Moscow, TsNINatominform, Part 4 (1980) 270 (in Russian).

[5] ANDREEV, O.L., et al., Annals of USSR Metrological Institutes 145(205) (1973) 33 (in Russian).

[6] YuDIN, M.F., et al., Measurement Techniques 4 (1985) 8 (in Russian).

[7] USSR INSTITUTE OF STANDARDS , "Measurements of Multiple Observation. Methods for the Processing of Measured Results", GOST 8.207-76, Moscow, Publication of Standards (1976) (in Russian).

[8] VONACH, H., Nuclear Data Standards for Nuclear Measurements, IAEA Technical Report Series No.227, IAEA, Vienna (1983) 59.

ANALYSIS OF ^{239}Pu PROMPT FISSION NEUTRON SPECTRA

S.Eh. Sukhikh, G.N. Lovchikova, V.A. Vinogradov, B.V. Zhuravlev,

A.V. Polyakov, O.A. Sal'nikov, Ch. Maerten (GDR), A. Ruben (GDR)

Abstract

The prompt ^{239}Pu neutron induced fission neutron spectrum has been measured at an incident neutron energy of 1.49 MeV. The measurements were carried out by means of the time-of-flight technique with a pulsed beam proton tandem accelerator and a tritium gas neutron source. Spectra were measured at 90° and 150° to the incident neutron beam. The use of the ^{252}Cf prompt neutron fission spectrum as a standard for the neutron detector efficiency calibration minimized the influence of the collimator channel zone and eliminated the need to take the spectrometer time scale calibration into account. The experimental results were compared with the generalized Madland-Nix model to calculate prompt fission neutron spectra. The results of the calculation were in good agreement with the experimental results.

Lately, there has been a growing interest in prompt neutron fission spectra measured at various fission inducing neutron energies. For many practical applications, the average neutron fission spectrum energy and its dependence on the initial energy, is a very important parameter particularly because of the effect it has on the breeding of nuclear reactor fuel. Until now, the majority of neutron fission spectra have been measured at thermal neutron energies. There are few data in the MeV energy range but they do not seem to exhibit any systematic behavior. It is not surprising, therefore, that the IAEA Consultants' Meeting on the physics of fission neutron emission (Japan 1988), emphasized the importance to have fission spectra measured at various energies. The limited amount of information on fast neutron induced fission spectra is due principally to the experimental difficulties encountered in such measurements. These depend on the difficulty to separate fission spectrum neutrons from neutrons emitted by concurrent reactions or by fissionable material present in the fission chamber used in such measurements. For instance, there are only three measurements [1,2 and 3] that report the investigation of prompt neutron fission spectra for plutonium at

incident neutron energies ranging from 1 to 10 MeV. The limited amount of information on fast neutron fission spectra has hindered the performance of detailed comparisons of experimental data with data determined theoretically which could improve the use of theory.

DESCRIPTION OF THE MEASUREMENTS AND FINAL RESULTS

The neutron fission spectra mesurements described in this report have been carried out with a time-of-flight spectrometer and a EhGP-10M accelerator operating in a pulsed mode. The neutrons were provided by the $T(p,n)^3He$ reaction from a tritium gas neutron source. The incident neutron energy was equal to 1.49±0.04 MeV. The structural details and characteristics of the neutron source are described in reference [4]. The average proton current incident on the target was 1 mA with a pulsed frequency of 5 MHz. The metallic plutonium sample, consisting of a hollow cylinder with an outer diameter of 4.5 cm, an inner diameter of 4.0 cm and a height of 4.8 cm, enclosed in a stainless steel container, was located 16.9 cm from the center of the gas target at an angle of 0^0 to the direction of the proton beam. The neutrons were detected by a scintillation counter located 198 cm from the center of the sample. The detector, consisting of a stilbene crystal (having a diameter of 6.3 cm and a height of 3.9 cm) in contact with an FEhU-30 photomultiplier, was placed in a shielding assembly described in refernce [5]. The absolute neutron detection efficiency was determined by comparing the measured prompt neutron spectrum with the calculated ^{252}Cf prompt neutron spectrum. The calculated spectrum was represented by a Maxwellian distribution with T=1.42 MeV corrected by the $\mu(E)$ function as recommended in reference [6]. The detector efficiency curve was calculated using the single scattering model for the interaction of neutrons with the stilbene crystal with the aid of the computer program described in reference [7]. The neutron detection threshold was equal to 0.6 MeV. The time resolution of the spectrometer was 3 ns at half-height of the gamma ray peak emitted by the target. The channel width of the time analyzer was equal to 0.503 ns, the integral non-linearity was 0.4% and the differential non-linearity was 0.6%. A scintillation detector, used to monitor

the neutron flux, also measured the time dependence of neutrons emitted by the target. The target neutron yield was monitored by a long counter. The schematic and the mode of operation of the electronic instrumentation is described in reference [8].

The experiment consisted of measurements of neutron spectra emitted by ^{239}Pu at angles of 90° and 150°. The experimental procedure consisted in neutron spectrum measurements of the Pu sample enclosed in the container and measurements of the background from the container alone at equal neutron flux intensities. Multiple measurements were performed in order to eliminate the effect of instabilities of the accelerator and of the electronics on the measurements. The stability of the conditions during the experiment was monitored by observing the shape and position of the monitored neutron spectrum peak, as well as the shape of the spectrum of neutrons emitted by the target at 0°.

The neutron spectrum emitted by the target at an angle of 0° with respect to the proton beam was measured during each measurements series. The absolute values of the differential cross-sections for the interaction of neutrons with ^{239}Pu nuclei were determined by normalization to the elastic scattering crosss-section for carbon measured at an angle of 90° to the direction of the incident neutron beam. The carbon scatterer consisted of a hollow graphite cylinder with an outer diameter of 3.0 cm, a height of 4.5 cm and a wall thickness of 0.5 cm containing 2.367 moles of ^{12}C. The value of the differential elastic scattering cross-section for carbon at an angle of 90° (in the laboratory system), equal to 0.152 b/sr, was taken from reference [8]. Only those neutrons which resulted from fission events in the energy interval of 2 to 10 MeV interval were included in the processing of the neutron spectra. The data processing is described in detail in reference [10]. The spectral measurements were corrected for the time resolution of the spectrometer [11] and for the attenuation and multiple scattering of neutrons in the sample which were derived from Monte Carlo calculations using the BRAND computer programs. The experimental neutron spectra measured at 90° and 150°, which are given in Fig.1, show that the cross-section values for neutrons emitted at 150° have a systematically higher value than those emitted at 90°.

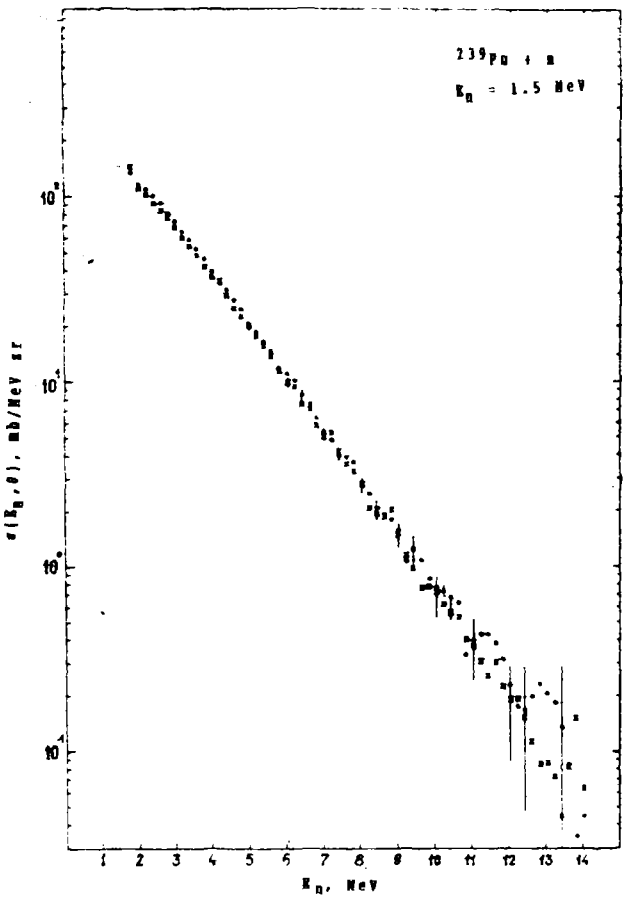

Fig. 1. Experimentally determined spectra for 90° and 150° angles:

■ 90° , O 150°

ANALYSIS OF THE EXPERIMENTAL DATA

Maxwellian Parametrization of the Neutron Spectra

In analyzing the ^{239}Pu prompt fission neutron spectra it was assumed that its shape can be described by a Maxwellian distribtion over most of its width given by

$$N(E) = C\sqrt{E}\,\exp\left(-\frac{E}{T}\right) \qquad (1)$$

where N(E) = number of neutrons in a unit energy interval,
E = neutron energy in MeV, and
C and T = distribution parameters.

Values for the T parameter were obtained by approximating the experimental data by a Maxwellian distribution using the least squares method in the energy interval from 2 to 10 MeV for the following two neutron emission angles:

T = 1.37 MeV for θ = 90°
T = 1.37 MeV for θ = 150°

The C and T parameters for the integral spectrum determined on the assumption of a symmetrical angular distribution of the prompt fission neutrons with respect to 90° relative to the direction of the incident neutrons, are equal to 4.54 $MeV^{3/2}/b$ and 1.37 MeV respectively. The value of T = 1.41±0.05 MeV in the energy interval of 2.8 to 6.5 MeV, for an incident neutron energy of 1.5 MeV, which was published in reference [2] is in good agreement with the results of this experiment within the limits of the experimental error. The ratio of the integral neutron fission spectrum to the calculated spectrum using the Maxwellian distribution with T = 1.37 MeV, is shown in Fig. 2.

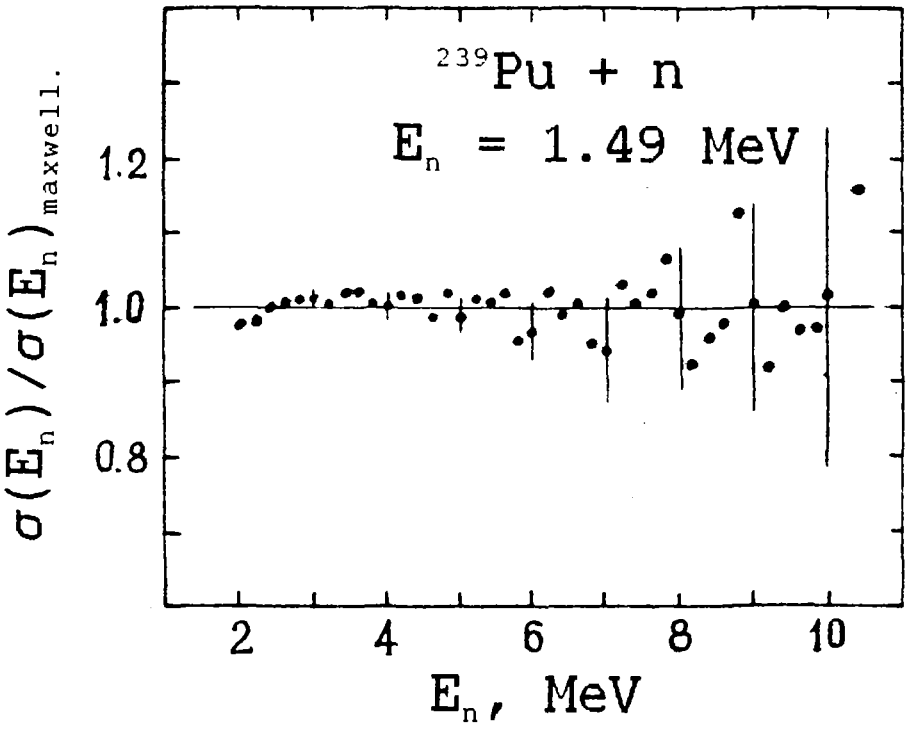

Fig.2. Ratio of the integral spectrum to the calculated Maxwellian spectrum with T = 1.37.

The magnitude of the ^{239}Pu fission neutron emission cross-section obtained by integrating the Maxwellian distribution using the parameters derived from the integral experimental spectrum is equal to 6.43±0.45 barns, i.e.

$$\int_0^{\infty} C\sqrt{E}\,\exp(E/T)\,dE = \sigma_f(E_0)\,\bar{\nu}_p(E_0) = 6.43 \qquad (2)$$

On the other hand, if one multiplies the evaluated value of σ_f (1.5 MeV), equal to 1.935 barns [13], with the measured value of $\bar{\nu}_p$ (1.5 MeV), equal to 3.078±0.021 [14], one obtains the value

of 5.955 b for the neutron emission cross-section which agrees satisfactorily with the results based on the measured spectrum.

The angular dependence of the number of ^{239}Pu fission neutrons is evaluated by comparing the number of neutrons detected at 150^0 and 90^0 with respect to the direction of the incident neutron beam. The ratio of the number of detected fission neutrons emitted at an angle of 150^0 to the number of neutrons emitted at an angle of 90^0 is equal to 1.06±0.02.

The angular dependence of prompt fission neutrons spectra can be influenced by the anisotropy of the emitted fission fragments with respect to the direction of the incident neutrons and by the anisotropy of neutrons emitted by those fragments which have attained their maximum velocity in the laboratory system. According to reference [15], the angular distribution of prompt fission neutrons with respect to the direction of those neutrons which induce the fission reaction can be described by the following equation:

$$W_n(\psi) = \sum_{i=0}^{2} A_i B_i \left[\frac{2}{2i+1}\right] P_i(\cos\psi) \qquad (3)$$

where - $W(\psi)$ is the number of fission neutrons emitted at an angle ψ;

- A_i and B_i are Legendre coefficients for the angular distributions of the fission fragments and of the neutrons emitted by the moving fragments, respectively, and

- $P_i(\cos\psi)$ are the Legendre polynomials.

The values of the A_i Legendre polynomial coeffficients for the angular distribution of the fission fragments with respect to the direction of the incident neutrons, which were calculated on the basis of ^{238}Pu measurents reported in reference [16], are: $A_0 = 1$, $A_1 = 0$, and $A_2 = 0.098$. The values of the B_i coefficients were taken from experimental angular distribution data for prompt neutrons from spontaneous fission of ^{252}Cf with respect to a fixed direction of fragment scatter [17], and are equal to $B_0 = 0.533$, and $B_2 = 0.666$. Substituting the values of these coefficients in equation (3), one obtains the following equation

$$W_n(\psi) = 1.066 + 0.026 \cdot P_2(\cos\psi)$$

which leads to the following ratio:

$$W_n(150^0) \;/\; W^n(90^0 = 1.03 \pm 0.01$$

Within the limits of the experimental uncertainty, this value is in good agreement with the measured value of this quantity. Values for the $N(150^0)/(90^0)$ ratio for a few prompt fission neutron energy intervals ΔE are given in the Table below.

Angular distribution for given energy interals

ΔE, MeV	$N(150^0)/(90^0)$ exp	$N(150^0)/(90^0)$ calc
2 - 4	1.07±0.02	1.035
4 - 6	1.05±0.05	1.051
6 - 8	1.06±0.04	1.055
8 - 10	1.05±0.07	1.060

COMPARISON OF THE EXPERIMENTALLY DETERMINED SPECTRA WITH THEORETICAL CALCULATION

Because of the complexity of the fission process, the approximation of the neutron fission spectrum by a Maxwellian or a Watt distribution is often inadequate. The development of theoretical models, or the improvement of existing ones, to calculated spectra of prompt fission neutrons is therefore extremely important. Currently, there exist three approaches for the calculation of prompt fission neutron spectra which use various approximations [18-20]. One of these is the generalized Madland-Nix model. This model allows one to calculate neutron spectra for any fissionable nucleus and excitation energy. The primary prompt neutron emission mechanism incorporated in this model is based on the evaporation of neutrons from all of the accelerated fission fragments. The generalized model differs from the simple Madland-Nix model in that the maximum temperature and the inverse reaction cross-section are a function of the mass numbers of each individual fragment. The fission neutron

spectrum is represented in the generalized Madland-Nix model by the following expression:

$$\varphi(E,\theta;A,Z,TKE) = \sum_I \sum_I \int dE^* f(P) f(\varphi) \qquad (4)$$

where

$$f(p) = P(E^*,I;A,Z,TKE)$$

and

$$f(\varphi) = \varphi_I(\varepsilon,\theta;E^*,I,A,Z)$$

and where for each fragment

E'	is the excitation energy,
A and Z	are the mass number and the charge,
TKE	is the total kinetic energy, and
I	is the spin.

Summing this expression over i results in an expression representing cascade evaporation. The f(P) function represents the distribution of the fission fragments as a function of masses, spins and energies. The model parameters used to describe neutron induced fission were taken from the data which characterizes the ^{252}Cf spontaneous fission neutron spectrum.

The basic input data used in the calculation of neutron fission spectra with the generalized Madland-Nix model are the average kinetic energies and the excitation energies of the fission fragments as a function of their mass number. These data were calculated using the double spheroid model taking shell corrections into account [21], which is based on the overall energy balance. The comparison of the calculated prompt neutron fission spectrum with the experimentally determined spectrum is shown in Fig. 3. The good agreement between experiment and theory to describe the distribution of neutrons substantiates the chosen approach in the application of the above mentioned theoretical models to give a good description of the fundamental characteristics of the process of neutron emission from fission fragments.

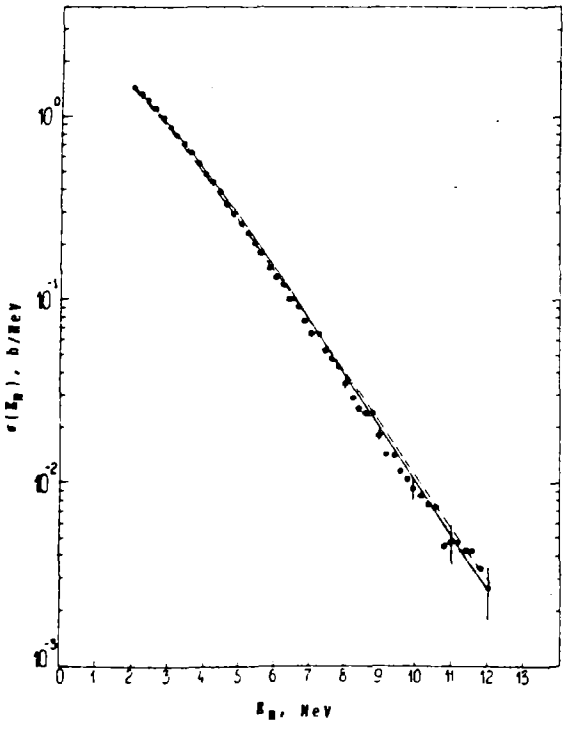

Fig. 3. Comparison of the calculated and experimentally determined prompt neutron fission spectrum:

- results of this experiment ●
- theory ————————

CONCLUSIONS

This experiment consisted in the measurement of prompt ^{239}Pu fission neutron spectra induced by 1.49 MeV neutrons, and measured at 90° and 150° with respect to the direction of the incident neutrons. The Maxwellian distribution parameters fitted to the experimentally determined spectra are in good agreement with results of other authors, and the value of the fission neutron emission cross-section agrees with the evaluated value based on the fission cross-section and the measured average number of neutrons per fission. The angular distributions of the prompt fission neutron spectra which were was derived in this work are not at variance with experimentally determined angular distributions of fission fragments and of neutrons emitted by the moving fission fragments.

This work also includes a comparison of experimentally determined spectra with theoretical calculations using the generalized Madland-Nix model and the double spheroid model. The good agreement between the measured and theoretical data confirms that the application of these theoretical models give a good description of the fundamental characteristics of the process of neutron emission from fission fragments.

REFERENCES

[1] SMITH, A.B., in Proc. Prompt Fission Neutron Spectra, IAEA, Vienna (1972) 3.

[2] KNITTER, H.H., COPPOLA, M., ISLAM, M.M., et al., ibid., p.41 .

[3] JOHANSSON, P.I., et al., (Proc. Internatiomal Conference on Nuclear Cross-Sections and Technology, Washington, DC, 1975), NBS Special Publication 425, Vol.2 (1975) 572.

[4] FETISSOV, N.I., SIMAKOV, S.P., TRUFANOV, A.M., et al., Experimental Instruments and Techniques, 6 (1980) 22 (in Russian).

[5] TRUFANOV, A.M., NESTERENKO, V.S., FETISSOV, N.I., et al., ibid., 2 (1979) 50 (in Russian).

[6] GRUNDL, J.A., EISENHAUER, C.M., (Proc. International Conference on Nuclear Cross-Sections and Technology, Washington, DC, 1975), NBS Special Publication 425, Vol.1 (1975) 250.

[7] TCHULKOV, L.V., "Computer program for the calculation of the detection efficiency of neutrons in stilbene", Institute of Atomic Energy, Moscow, Preprint IAE-2594 (1976) (in Russian).

[8] SIMAKOV, S.P., LOVCHIKOVA, G.N., TRUFANOV, A.M., et al., Atomnaya Ehnergiya 51 4 (1981) 244 (in Russian).

[9] BYCHKOV, V.M., KORNILOV, N.V., PASHCHENKO, A.B., SKRIPOVA, M.V., "Nuclear reaction cross-sections recommended to be used as standards in neutron measurements", FEI, Obninsk, Preprint FEI-1917 (1988) (in Russian).

[10] LOVCHIKOVA, G.N., POLYaKOV, A.V., SAL'NIKOV, O.A., et al., "Investigation of neutron spectra emitted by ^{232}Th and ^{234}U bombarded by 6 MeV neutrons", FEI, Obninsk, Preprint FEI-1564 (1984) (in Russian).

[11] MAERTEN, H., et al., IAEA report INDC(GDR)-28/L (1984).

[12] ANDROSSENKO, A.A., ANDROSSENKO, P.A., Problems of Atomic Science and Technology. Ser. Physics and Technology of Nuclear Reactors 7 (1985) 33 (in Russian).

[13] ANTSIPOV, G.V., BAKHANOVICH, L.A., ZHARKOV, V.F., et al., "Evaluation of the ^{239}Pu nuclear data", A.B. Lykov Heat- and Mass-Transfer Institute, BSSR Academy of Sciences, Minsk, Preprint-14 (1982) (in Russian).

[14] MALINOVSKIJ, V.V., TARASKO, M.Z., KUZ'MINOV, B.D., Atomnaya Ehnergia 58 6 (1985) 430 (in Russian).

[15] BIRYuKOV, N.S., ZHURAVLEV, B.V., KORNILOV, N.V., et al., Problems of Atomic Science and Technology. Ser. Nuclear Constants 12 1 (1973) 48 (in Russian).

[16] SHPAK, D.L., OSTAPENKO, Yu.B., SMIRENKIN, G.N., Yadernaya Fizika XIII 5 (1971) 950 (in Russian).

[17] BOLDEMAN, H.R., MILTON, J.C.D., THOMPSON, S.G., SWIATECKI, W.J., Phys.Rev. 129 5 (1963) 2133.

[18] MAERTEN, H., SEELIGER, D., Nucl. Sci. Eng. 93 (1986) 370, and MAERTEN, H., (Proc. IAEA Advisory Group Meeting on the Properties of Neutron Sources, Leningrad 1986) Rep. IAEA-TECDOC-410 (1987) 153.

[19] MADLAND, D.G., NIX, J.R., Nucl. Sci. Eng. 81 (1982) 213.

[20] GERASSIMENKO, B.F., RUBCHENYA, V.A., Bulletin of Nuclear Data Centre 12 (1986) 3.

[21] TERREL, J., Proc. (IAEA Symposium on the Physics and Chemistry of Fission, Salzburg 1965), IAEA, Vienna Vol. 2 (1965) 3.

MEASUREMENT AND EVALUATION OF THE $^{64}Zn(n,p)^{64}Cu$, $^{90}Zr(n,2n)^{89}Zr$ AND $^{111}Cd(n,n')^{111m}Cd$ REACTION CROSS-SECTIONS AVERAGED OVER THE ^{235}U FISSION NEUTRON SPECTRUM

E.I. Grigoryev, Yu.A. Melekhin, V.S. Troshin, V.P.Yarina

Abstract

The cross-sections for the $^{64}Zn(n,p)^{64}Cu$, $^{90}Zr(n,2n)^{89}Zr$ and $^{111}Cd(n,n')^{111m}Cd$ reactions averaged over the ^{235}U fission neutron spectrum have been measured. The results of these measurements are 34.4±0.8 mb, 0.0945±0.0045 mb and 198±4 mb, respectively. The absolute intensity of the 0.52 MeV ^{64}Cu photon was taken to be 0.343. The evaluated values for zinc and zirconium were 33.8±0.7 mb and 0.0966±0.0024 mb respectively. The cadmium reaction cross-section was not evaluated as there are no other published results.

The investigation of these reactions are of practical interest as they are used in the spectrometric neutron activation measurements of reactor neutron fields. In such applications, the basic criterion used to determine the suitability of given reaction cross-sections is whether their integral (or average) activation cross-sections had been measured in known neutron fields and calculated for these fields as a function of neutron energy using differential reaction cross-sections.

The aim of this work consisted in obtaining reliable average cross-section data for the chosen reactions measured in a ^{235}U fission neutrons spectrum, and their subsequent choice based on their agreement with the differential cross-sections values.

The experimental determination of the average reaction cross-sections induced by ^{235}U fission neutrons was performed in accordance with the method described in reference [1], taking into account results of measurements in distinct neutron fields of water-water reactors having well-defined standard ^{235}U fission neutron spectrum characteristics.

In these experiments, the reactor neutron field characteristics were measured with neutron activation detectors with the use of

reactions included in the RNMF-87 data file, whose cross-sections are recognized as standard reference data (SRD) [2]. Some of the threshold reactions and their cross-sections for the ^{235}U and ^{252}Cf fission neutrons, calculated with the use of the SRD, are given in Table 1. In this experiment the average reaction cross-sections were measured relative to the complete set of cross-sections included in the RNMF-87 file.

Table 1. Average reaction cross-sections for ^{235}U and ^{252}Cf fission neutrons taken from the RNMF-87 File

Reactions	Average Cross-Sections, mb	
	^{235}U	^{252}Cf
$^{19}F(n,2n)^{18}F$	0.0079	0.0166
$^{24}Mg(n,p)^{24}Na$	1.453	2.120
$^{27}Al(n,\alpha)^{24}Na$	0.6961	1.039
$^{32}S(n,p)^{32}P$	63.29	71.30
$^{54}Fe(n,p)^{54}Mn$	78.80	90.40
$^{56}Fe(n,p)^{56}Mn$	1.039	1.454
$^{58}Ni(n,p)^{58}Co$	102.8	116.9
$^{93}Nb(n,2n)^{92m}Nb$	0.4385	0.7833
$^{103}Rh(n,n')^{103m}Rh$	729.0	756.0
$^{115}In(n,n')^{115m}In$	187.0	195.7
$^{204}Pb(n,n')^{204m}Pb$	19.71	23.67
$^{237}Np(n,f)$	1327	1351

The radioactive decay properties of the reaction products resultimg from the investigated reactions, which were used in the processing of the measured results, are listed in Table 2, and the average reaction cross-sections in different neutron fields are tabulated in Table 3.

The evaluated experimental results are considered as average weighted values for the set of measured values. The uncertainty of the evaluated results consisted of the root-mean-square errors and a general systematic error for each individual value.

Table 2. Decay properties of reaction products

Nuclide	Half-life	Photon energy MeV	% Absolute intensity
^{64}Cu	12.701 h	0.511 1.34	34.3 0.47
^{89}Zr	3.268 d	0.910	99
^{111m}Cd	48.7 m	0.151 0.245	30.3 94.2

Table 3. Measured reaction cross-sections averaged over the ^{235}U spectrum (data given in mb).

^{64}Zn(n,p)^{64}Cu	^{90}Zr(n,2n)^{89}Zr	^{111}Cd(n,n')^{111m}Cd
35.5±1.7	0.094±0.006	195±9
33.5±1.6	0.098±0.006	196±8
33.6±1.3	0.093±0.005	203±10
32.2±1.2	0.093±0.006	-
34.5±1.4	-	-
35.7±1.7	-	-
35.5±1.8	-	-
34.4±0.8	0.0945±0.0045	198±4

Although the ^{64}Zn(n,p)^{64}Cu reaction is used extensively in neutron activation spectrometry, the values of the measured differential cross-sections as well as of the average cross-sections found in the literature differ considerably from each other. One of the reason for these discrepancies could be due to the use of various values of the absolute intensity of the ^{64}Cu 0.511 MeV gamma ray.

The values that have been used for this quantity are: 0.38, 0.357, 0.368, and 0.343. The value of 0.343, which is associated with the reaction cross-section value of 4.50 b for the ^{63}Cu(n,γ)^{64}Cu reaction at thermal neutron energies, was used in this experiment and in the ensuing evaluation. The samples used in this experiment consisted of metallic disks of ^{64}Zn enriched to 99.5%, weighing anywhere from tens to hundreds of mg. During irradiation the samples were

covered with cadmium or small-sized boron shields having a ^{10}B density of 0.4 g/cm^2. The experimental results, as well as the evaluated average of the measured cross-sections are tabulated in Table 4.

Table 4. Evaluation of the $^{64}Zn(n,p)^{64}Cu$ Reaction Cross-Section Averaged over the ^{235}U Fission Spectrum

LEGEND

Column A: Reference
Column B: $\bar{\sigma}$, mb quoted in reference
Column C: Absolute intensity of the 0.511 MeV photon
Column D: $\bar{\sigma}$, mb normalized to 0.343 absolute intensity
Column E: standard used in reference
Column F: Normalization factor
Column G: Normalized $\bar{\sigma}$, mb

A	B	C	D	E	F	G
[4]	27.0±2.4	0.38	29.9	Fe(67)	1.175	35.1±3.2
[5]	30.1±0.8	0.38	33.4	Al(0.705)	0.987	32.9±0.9
[6]	27.0±1.6	0.38	29.9	*	1.11	33.2±2.0
[7]	29.9±1.6	0.38	33.1	Al(0.705) (108.5)	0.967	32.0±1.7
[8]	26.9±1.2	0.38	29.8	Ni(95)	1.082	32.3±1.5
[9]	32.4±1.0	0.368	34.7	In(187)	1.00	34.7±1.1
[10]	30.9±2.1	**	32.9	*	1.05	34.5±2.3
***	34.4±0.8	0.343	34.4	-	-	34.4±0.8

Final evaluated value: $\bar{\sigma}$ = 33.8±0.6 mb

Annotations: * the normalization factor was determined using all average reaction cross-section values which were used by the author in his experiment.

** the 1.34 MeV gamma ray which has an absolute intensity of 0.5% was used in this experiment, the result was recalculated for an absolute intensity of 0.47%.

*** result of this experiment.

The procedure followed to obtained the evaluated average reaction cross-section, based on the full set of published data, consisted of the following steps:

- reduction of all results to the same decay characteristics of the reaction product,
- normalization of results to the same calibration standard (average reference reaction cross-section) or, when this was not possible, determination of a common normalizing factor based on all of the reaction cross-sections which were used by the author in a given experiment,
- determination of a weighted average value for the determined results,
- determination of the error of the evaluated average cross-section value.

The value of the decay properties used in the normalization of the data are listed in Table 2. The values of the weighted average cross-sections for a number of $\bar{\sigma}_i$ having their own uncertainties were calculated using the following equation:

$$\bar{\sigma} = \frac{\sum_i p_i \cdot \bar{\sigma}_i}{\sum_i p_i}$$

where $p_i = 1/S_i$ is the weight of the ith average cross-section.

The root-mean-square error (rms) for the given set of values was determined from:

$$S_p = \sqrt{\frac{\sum_i p_i \cdot (\bar{\sigma} - \bar{\sigma}_i)^2}{(n-1) \cdot \sum_i p_i}}$$

where n is the total number of values in the set. The uncertainty of the evaluated δ in the form of the rms error was determined from

$$S = \sqrt{S_p^2 + \tfrac{1}{3}\theta^2}$$

where θ is the common systematic error for all of the values in the set.

Of all the standard reactions available in the literature, the following were used in this exercise: $^{27}Al(n,\alpha)^{24}Na$, $^{54}Fe(n,p)^{54}Mn$,

$^{58}Ni(n,p)^{58}Co$, and $^{115}In(n,n')^{115m}In$; the values of these cross-sections, averaged over the ^{235}U spectrum, are listed in Table 1. In the tabulations of the evaluated data, these standards are designated by the symbol of the element used as standard, and the value of the averaged cross-sections used by the authors of this work are given in paretheses.

The results of the evaluation of the averaged $^{64}Zn(n,p)^{64}Cu$ reaction are given in Table 4. The tabulated information consists of: the source reference, the result obtained by the author, the value of the absolute intensity of the 0.511 MeV gamma ray used by the author, the value of the averaged cross-section normalized to the absolute intensity of 0.343, the standard used by each author, the normalization factor used in the evaluation, and in the last column the final values of the normalized averaged cross-sections.

The set of experimental results of the $^{90}Zr(n,2n)^{89}Zr$ reaction cross-sections averaged over the ^{238}U spectrum, assembled in reference [3], was not considered to be suitable for evaluation. However,

Table 5. Evaluation of the $^{90}Zr(n,2n)^{89}Zr$ reaction cross-section averaged over the ^{235}U fission spectrum.

LEGEND

Column A: Reference
Column B: $\bar{\sigma}$, mb qoted in the reference
Column C: standard used in reference work
Column D: normalizing factor
Column E: final normalized $\bar{\sigma}$ value in mb

A	B	C	D	E
[11]	0.1044±0.0046	Al(0.725) M(0.258)	0.947	0.0989±0.0044
[12]	0.103±0.004	(109)	0.943	0.0971±0.0038
[3]	0.096±0.006	-	-	0.096±0.006
***	0.0943±0.0045	-	-	0.0945±0.0045

Evaluate value: $\bar{\sigma}$ = 0.0966 ± 0.0024 mb

Annotation: *** result of this experiment

the data published in references [11] and [12] together with the data measured in this experiment were evaluated, and produced an average value for the averaged cross-section of this reaction.

The results given in Table 5 also confirm the conclusion presented in reference [3], that the cross-section dependence given in reference [2], is suitable for neutron activation spectrometry.

Inasmuch as there are no published data on the averaged $^{111}Cd(n,n')^{111m}Cd$ reaction cross-section, it is recommended that the value of 198±4 mb, obtained in this work, be used as such.

The recommended integral cross-section values averaged over the ^{235}U fission spectrum, and the associated effective cross-sections applicable to a wide class of reactor spectra cited in the BKS-2 data library [3], and the maximum spread θ_{eff} of the recommended value of the effective cross-section for actual spectra of various reactors are given in Table 6.

Table 6. Recommended integral Cross-sections

Reaction	$\bar{\sigma}$, mb	E_{eff}, MeV	σ_{eff}, mb	θ_{eff}, %
$^{64}Zn(n,p)$	33.8±0.7	3.0	162	4
$^{90}Zr(n,2n)$	0.0966±0.0024	13.3	919	1
$^{111}Cd(n,n')$	198±4	1.3	350	2.5

REFERENCES

[1] GRIGORYEV, E.I., TARNOVSKIY, G.B., YARYNA, V.P.,(Proc. Sixth All-Union Conference on Neutron Physics, Kiev, 1983), TsNIIatominform, Vol. 2 (1984) 187 (in Russian).

[2] USSR GSSSD PUBLISHER, Neutron Activation Detectors for Reactor Measurements. "Reaction Cross-sections for the Interaction of Neutrons with Nuclei. RNMF-87: Tables of Standard Reference Data" (1988) (in Russian).

[3] GRIGORYEV, E.I., MELEKHIN, Yu.A., YARYNA, V.P., Problems of Atomic Science and Technology. Ser. Nuclear Constants 3 (1987) 27 (in Russian).

[4] NASSYROV, F., Atomnay Ehnergia 25 5 (1968) 437 (in Russian).

[5] NAJZER, M., RAUT, J., (Proc. Advisory Group Meeting on Neutron Cross-sections for Reactor Dosimetry, IAEA, Vienna), Rept. IAEA-208, Vol.2 (1978) 247.

[6] BOLDEMAN, I.W., J. Nucl. Energy 18 8 (1964) 247.

[7] FABRY, A., et al., (Proc. Advisory Group Meeting. on Neutron Cross-sections for Reactor Dosimetry, IAEA, Vienna), Rept. IAEA-208, Vol.2 (1978) 233.

[8] RAU, G., Nukleonics 9 (1967) 228.

[9] HANNAN, Ah.A., WILLIAMS, U.G., (Proc. Advisory Group Meeting on Neutron Cross-sections for Reactor Dosimetry, IAEA, Vienna), Rept. IAEA-208, Vol.2 (1978) 209.

[10] KOBAYASHI, K., et al., Nucl. Sci. and Technol. 3 (1976) 531.

[11] SEKINE, T., BOBA, H., Inorg. Nucl. 43 7 (1981) 427.

[12] MANHART, W.,(Proc. Symp. on Reactor Dosimetry, IAEA, Geesthacht) IAEA Rept. Vol.2 (1984) 813.